European Journal of Medicinal Chemistry 124 (2016) 677–688

Contents lists available at ScienceDirect

European Journal of Medicinal Chemistry

journal homepage: http://www.elsevier.com/locate/ejmech

Research paper

Translocator protein ligands based on *N*-methyl-(quinolin-4-yl) oxypropanamides with properties suitable for PET radioligand development

Chad Brouwer, Kimberly J. Jenko, Sami S. Zoghbi, Cheryl L. Morse, Robert B. Innis, Victor W. Pike*

Molecular Imaging Branch, National Institute of Mental Health, National Institutes of Health, Building 10, Room B3 C346A, 10 Center Drive, Bethesda, MD 20892, United States

ARTICLE INFO

Article history:
Received 8 June 2016
Received in revised form
28 July 2016
Accepted 21 August 2016
Available online 25 August 2016

Keywords:
Translocator protein
PET
Carbon-11
Ligand
Binding affinity
Lipophilic efficiency

ABSTRACT

Modifications to an *N*-methyl-(quinolin-4-yl)oxypropanamide scaffold were explored to discover leads for developing new radioligands for PET imaging of brain TSPO (translocator protein), a biomarker of neuroinflammation. Whereas contraction of the quinolinyl portion of the scaffold or cyclization of the tertiary amido group abolished high TSPO affinity, insertion of an extra nitrogen atom into the 2-arylquinolinyl portion was effective in retaining sub-nanomolar affinity for rat TSPO, while also decreasing lipophilicity to within the moderate range deemed preferable for a PET radioligand. Replacement of a phenyl group on the amido nitrogen with an isopropyl group was similarly effective. Among others, compound **20** (*N*-methyl-*N*-phenyl-2-[2-(pyridin-2-yl)-1,8-naphthyridin-4-yloxy]propanamide) appears especially appealing for PET radioligand development, based on high selectivity and high affinity (K_i = 0.5 nM) for rat TSPO, moderate lipophilicity (log*D* = 2.48), and demonstrated amenability to labeling with carbon-11.

Published by Elsevier Masson SAS.

1. Introduction

Translocator protein 18 kDa (TSPO), formerly known as the peripheral benzodiazepine receptor [1], is located predominantly at the outer mitochondrial membrane in association with a voltage-dependent anion channel and an adenine nucleotide transporter [2]. TSPO is present in several major organs, and is particularly dense in adrenal gland, heart, kidney, and testis [2]. Low amounts are present in normal human brain, primarily in microglia [3]. Activated microglia upregulate TSPO in instances of neuronal damage [4] as seen in many neurological disorders [5–7] including Alzheimer's disease, movement disorders, stroke, multiple sclerosis, and major depression [8]. Therefore, TSPO can serve as an important biomarker for neuroinflammation. Moreover, ligands for TSPO have also been explored as possible drugs, particularly for anxiety [9].

For more than three decades, PET imaging of human TSPO has been carried out with [^{11}C]PK11195 ([^{11}C]**1**) [10] or its (*R*)-enantiomer ([^{11}C](*R*)-**1**) [11] (Chart 1) for biomedical investigations of neuroinflammation. [^{11}C](*R*)-**1** has been by far the most employed radioligand for this purpose despite limited brain uptake [12], low specific binding [12], and an undesirable metabolic profile [13]. Efforts to tackle these shortcomings of [^{11}C](*R*)-**1** have resulted in several new structural classes of TSPO radioligand with superior imaging characteristics (Chart 1). Examples include [^{11}C]PBR28 ([^{11}C]**2**) [14,15], [^{11}C]DAA1106 ([^{11}C]**3**) [16], [^{11}C]DPA-713 ([^{11}C]**4**) [17], [^{18}F]DPA-714 ([^{18}F]**5**) [18], [^{18}F]FBR ([^{18}F]**6**) [19], [^{18}F]PBR111 ([^{18}F]**7**) [20], [^{18}F]FEPPA ([^{18}F]**8**) [21], [^{18}F]FEMPA ([^{18}F]**9**) [22], and [^{11}C]ER176 ([^{11}C]**10**) [23]. Nonetheless, many of these new radioligands also suffer particular deficiencies, most prevalent of which is sensitivity to the rs6971 polymorphism in human subjects [20,21,24,25].

Successful PET radioligands for imaging specific proteins in brain are required to display a wide array of properties [26]. Among

Abbreviations: DIPEA, diisopropylethylamine; DMF, *N*,*N*-dimethylformamide; DMSO, dimethylsulfoxide; HFIP, hexafluoroisopropyl alcohol; HRMS-ESI, high resolution mass spectrometry electrospray ionization; LDA, lithium diisopropylamide; MTBE, methyl *tert*-butyl ether; PFP, pentafluorophenyl; PyBroP, bromotripyrrolidinophosphonium hexafluorophosphate; TEA, triethylamine; TSPO, translocator protein (18 kDa); LipE, lipophilic efficiency.

* Corresponding author.
E-mail address: pikev@mail.nih.gov (V.W. Pike).

http://dx.doi.org/10.1016/j.ejmech.2016.08.046
0223-5234/Published by Elsevier Masson SAS.

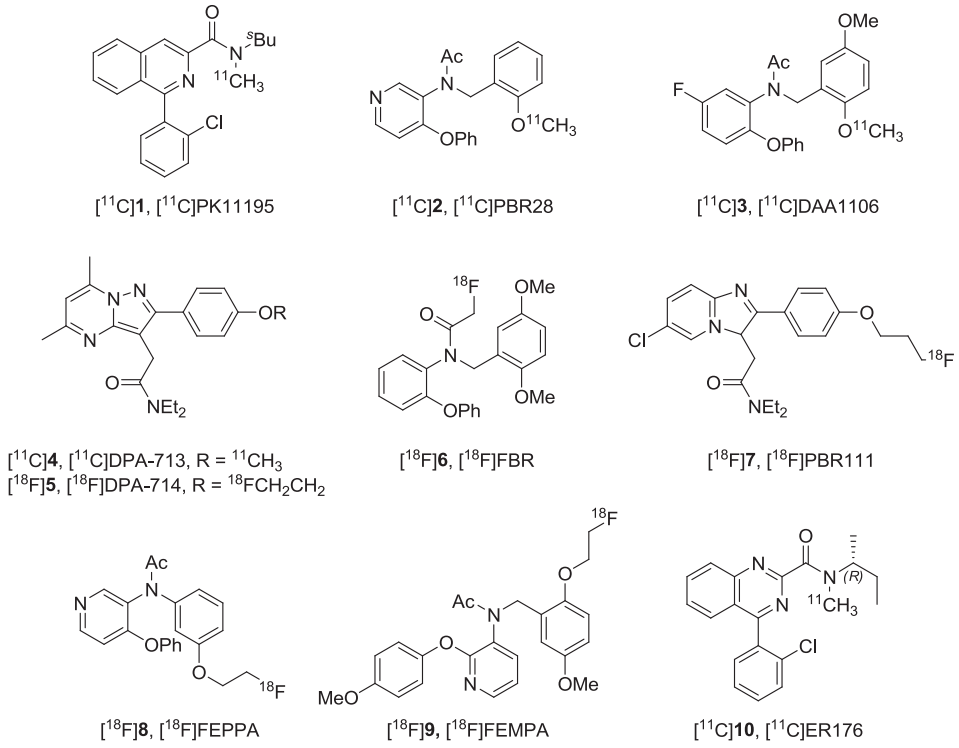

Chart 1. Structures of some notable TSPO PET radioligands.

these properties are: i) high affinity and selectivity for the target protein; ii) low molecular weight; iii) intermediate polar surface area for blood-brain barrier penetration; iv) moderate lipophilicity for adequate brain entry in the absence of excessive non-specific binding; and v) amenability to labeling with a positron-emitter, either carbon-11 ($t_{1/2}$ = 20.4 min) or fluorine-18 ($t_{1/2}$ = 110 min). This study aimed to develop TSPO ligands as leads with a desirable combination of properties for PET radioligand development. We have previously explored a series of *N*-methyl-(quinolin-4-yl)oxypropanamides as prospective TSPO ligands [27], and encouragingly many of these ligands have shown low TSPO genotype sensitivity in vitro. Here, we further explore structure-affinity relationships in this structural class. High-affinity TSPO ligands emerged from this effort and a few of these are promising new leads to PET radioligands.

2. Results and discussion

In this study, we identified new leads to PET radioligands for imaging TSPO based on modifications to the previously reported [27] *N*-methyl-(quinolin-4-yl)oxypropanamide TSPO ligand scaffold (Chart 2). These modifications were aimed at exploring, i) variation of substituents on the amide nitrogen, ii) introduction of nitrogen into the quinolin-4-yl group or pendant aryl ring, iii) replacement of the pendant aryl ring with methoxy, 2-pyrimidinyl or *N*-pyrrolidinyl, iv) the effect of cyclization to eliminate amide bond rotation, and v) contraction of the bicyclic quinolinyl nucleus. Generally, PET radioligands are required to have high affinity with K_D in the low nM range, and moderate lipophilicity with measured (or computed) logD in the 2–4 range [26]. Most of the changes that we made to the lead ligand scaffold were intended to retain the very high TSPO affinity (K_i = 0.07 nM for rat TSPO) seen in the previously reported example **11** (Chart 2; scaffold with Y = 2-pyridinyl, and R = Ph), as well as to decrease ligand computed lipophilicity (clog*D*) from 4.73 towards the desirable range. Usually, the overall shape of the scaffold was modified little to retain high affinity, although the effects of scaffold pruning were also investigated. The main strategy for lowering lipophilicity was to introduce nitrogen into one or more of the aryl rings. The lipophilicity cost for high ligand affinity may be indexed as a lipophilicity efficiency parameter (LipE), defined as ligand pIC_{50} (or pK_i) minus clog*D* [28]. Therefore, our overall aim encompasses the discovery of ligands with high LipE scores (>6). The amide *N*-methyl substituent was retained in all new ligands as a site that should be amenable to labeling with carbon-11 through ^{11}C-methylation of *N*-desmethyl precursors.

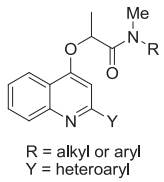

Chart 2. The *N*-methyl-(quinolin-4-yl)oxypropanamide scaffold used as a basis for new TSPO ligand development.

2.1. Chemistry

As prospective TSPO ligands, the 2-heteroaryl-4-alkoxyquinolines **18**–**23** (Scheme 1) were synthesized in three steps, proceeding with acylations of the requisite 2-amino-arylethanones [29]. The resultant amides **12** and **13** were subjected to Camps cyclization [30] to yield the 2-heteroarylquinolin-4-ones **14** and **15**, respectively, which were then chemoselectively *O*-alkylated to the desired ligands **18**–**23** (Scheme 1). The required α-bromoamides **16** and **17** were made under Schotten–Baumann conditions.

The 2,4-dialkoxy-1,8-naphthyridine ligand **27** was made by first

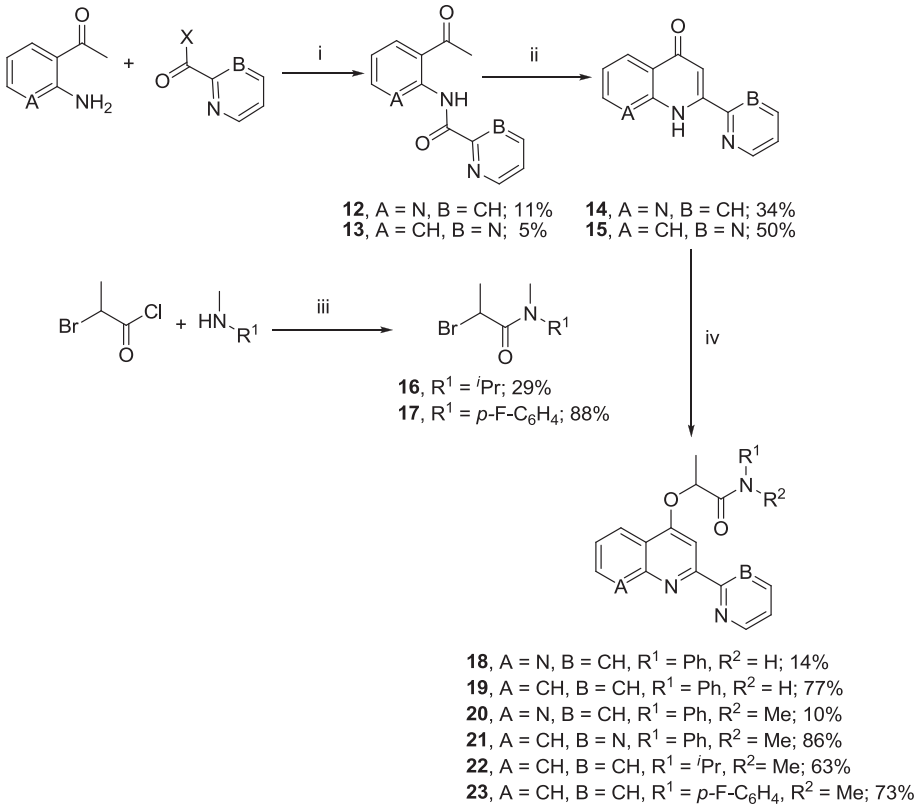

Scheme 1. Syntheses of 2-heteroaryl-4-alkoxyquinolines **18**–**23**. Reagents and conditions: (i) for **12** (X = Cl): TEA, $CHCl_3$, 4 °C; for **13** (X = ONa): DMF, DIPEA, PyBroP, CH_2Cl_2, rt; (ii) NaOH, dioxane, 110 °C; (iii) KOH, EtOAc, H_2O, 4 °C; (iv) for **18**: NaH, DMSO, 2-bromo-*N*-phenylpropanamide, 80 °C; for **19**: K_2CO_3, MeCN, 2-bromo-*N*-phenylpropanamide, 55 °C; for **20**–**21**; K_2CO_3, MeCN, 2-bromo-*N*-methyl-*N*-phenylpropanamide, 55–60 °C; for **22**–**23**: K_2CO_3, MeCN, **16**–**17**, 55–60 °C.

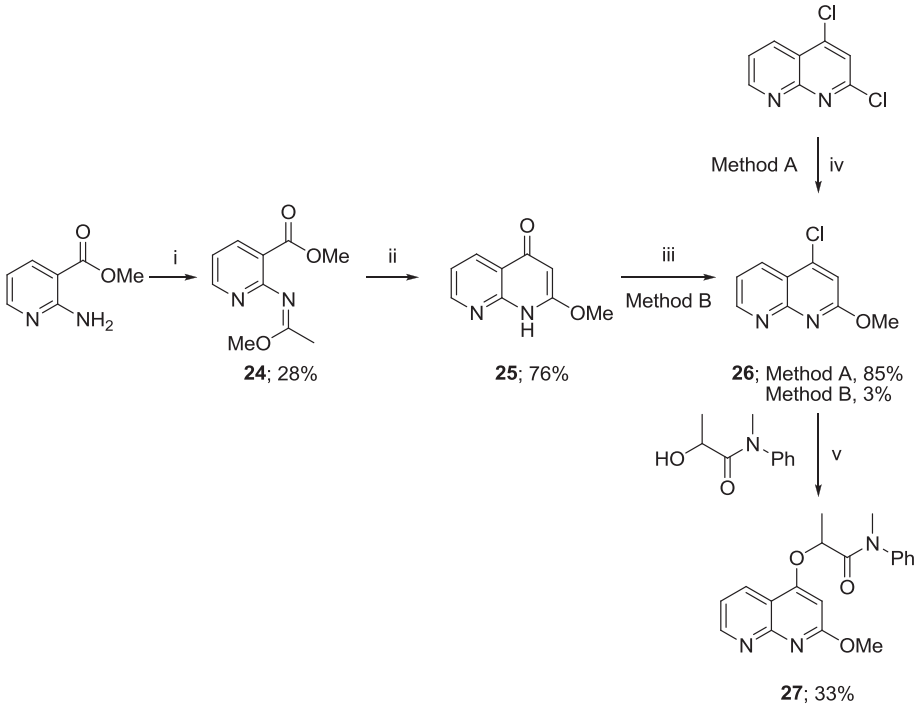

Scheme 2. Synthesis of the 2,4-dialkoxy-1,8-naphthyridine analog **27**. Reagents and conditions: (i) $MeC(OMe)_3$, Ac_2O, 110 °C; (ii) LDA, THF, hexane, −50 °C; (iii) $POCl_3$, 110 °C; (iv) NaOMe, toluene, rt; (v) NaH, DMF, DMSO, rt.

accomplishing a regioselective methoxylation [31,32] at C2 of 2,4-dichloro-1,8-naphthyridine to yield 2-methoxy-4-chloro-1,8-naphthyridine **26** (Method A, Scheme 2). The position of methoxylation was confirmed by an alternative but much lower yielding regiospecific synthesis wherein methyl 2-aminopyridine-3-carboxylate was first converted into the methyl acetimidate **24**. Dieckmann condensation [33] of **24** then gave 2-methoxy-1,8-naphthyridin-4-one **25**. Compound **25** was then converted into **26** by treatment with phosphoryl chloride (Method B, Scheme 2), but in only 3% yield. Finally, alkoxylation at C4 of **26** gave **27** (Scheme 2).

The 2-pyrrolequinoline ligand **29** was made by chemoselective *O*-alkylation [34] of 2-amino-4-hydroxyquinoline to yield **28** followed by treatment of its free base with dimethoxytetrahydrofuran in acetic acid (Scheme 3) [35].

Two analogs of ligand **22**, namely **33** and **34**, in which rotation of the amide bond was eliminated through cyclization, were synthesized in two steps. First, an appropriate lactam was subjected to α-chlorination with hexachloroethane to give compounds **31** and **32** in moderate yields [36,37]. Alkylation of 2-(pyridin-2-yl)-quinolin-4(1*H*)-one with each of these α-chlorolactams required prolonged heating but eventually gave the desired ligands **33** and **34**, respectively, in moderate yields (Scheme 4).

Finally, a ring-contracted analog of **11**, namely **36**, was made through nucleophilic amination [38] of 1-fluoro-2-nitrobenzene to yield 2-nitro-*N*-(pyridin-2-ylmethyl)aniline **35**, followed by treatment of **35** with two equivalents of sodium hydride to give the cyclized intermediate benzimidazole-*N*-oxide, and finally alkylation [39] of this oxide in situ with α-bromoamide **16** (Scheme 5).

2.2. Ligand pharmacology: TSPO binding affinity, cLogD, and LipE

The binding affinities ($1/K_i$) of all TSPO ligands, including the previously reported ligand **11**, were determined on rat brain homogenates (Table 1). We tested all ligands as racemates only, with the assumption that the high-affinity enantiomer has twofold higher affinity than that recorded for the racemate [27].

The *N*-(*p*-fluorophenyl) analog **23** of the previously described high-affinity TSPO ligand **11** maintained very high binding affinity and a comparably high LipE value (Table 1). Ligand **23** opens up the possibility to prepare an ^{18}F-labeled ligand, according to modern ^{18}F-labeling techniques [40,41].

Previously, we achieved an increase in LipE by introducing a nitrogen atom at either the 2′ position of the pendant phenyl group or the 8 position of the quinolinyl scaffold (Chart 2) [27]. We presumed that by having nitrogen atoms at both positions in the same ligand that we might significantly improve LipE, and, indeed, this turned out to be the case in ligand **20** (Table 1). We obtained a similar result when the pendant phenyl group alone was modified to have nitrogen atoms at positions 2′ and 6′, as in ligand **21** (Table 1). Previously, we had established the tolerance of the TSPO binding pocket for ligands containing nitrogen atoms at positions 2′, 3′, and 4′ of the pendant aryl group of the lead scaffold [27]. Nitrogen at the 1′ position in a pyrrolyl ring was no exception, yielding ligand **29** with high affinity (K_i = 0.22 nM) and high LipE

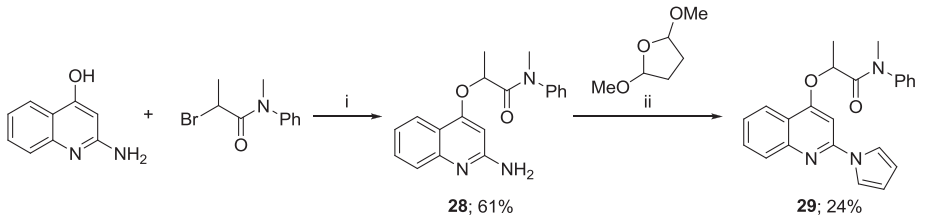

Scheme 3. Synthesis of 2-pyrrolequinoline analog **29**. Reagents and conditions: (i) NaOEt, EtOH, 70 °C, then α-bromoamide, DMF, 90 °C; (ii) AcOH, 120 °C.

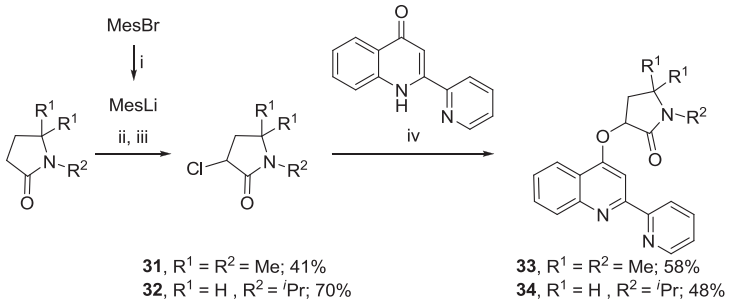

Scheme 4. Synthesis of α-quinolinyloxylactam analogs **33** and **34** with eliminated amide bond rotation. Reagents and conditions: (i) *t*-BuLi, pentane, THF, −60 to −70 °C, then −20 °C; (ii) THF, −70 °C, then 0 °C; iii) C_2Cl_6 THF, −78 to −70 °C, and then rt; (iv) K_2CO_3, MeCN, 80 °C.

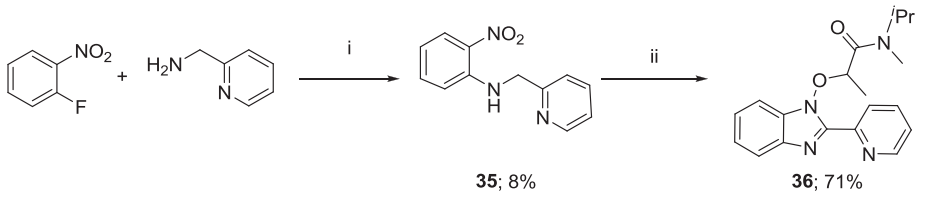

Scheme 5. Synthesis of ring-contracted analog **36**. Reagents and conditions: (i) K_2CO_3, DMF, 90 °C; (ii) **16**, NaH, DMF, 55 °C.

Table 1
K_i, clog*D* and LipE values for new oxypropanamide TSPO ligands; comparison with those of the classical ligand **1** and the progenitor ligand **11**.

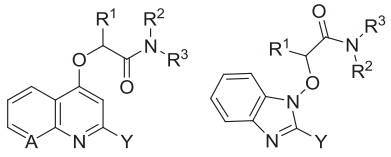

Ligand	A	Y	R^1	R^2	R^3	Rat K_i (nM)[a]	cLog*D*	LipE
1 (PK11195)[b]						0.5 ± 0.3	3.97	4.3 ± 0.2
11[b]	CH	2-Pyridinyl	Me	Me	Ph	0.10 ± 0.05	4.18 (3.11 ± 0.02)[c]	5.9 ± 0.2
20	N	2-Pyridinyl	Me	Me	Ph	0.5 ± 0.1	2.80 (2.48 ± 0.06)[c]	6.5 ± 0.1
21	CH	2-Pyrimidinyl	Me	Me	Ph	0.53 ± 0.08	2.71	6.6 ± 0.1
22	CH	2-Pyridinyl	Me	Me	^{i}Pr	0.76 ± 0.09	2.54	6.58 ± 0.05
23	CH	2-Pyridinyl	Me	Me	*p*-F-C_6H_4	0.09 ± 0.01	4.25	5.80 ± 0.06
27	N	OMe	Me	Me	Ph	7.8 ± 0.6	2.02	6.09 ± 0.04
29	CH	1-Pyrrolyl	Me	Me	Ph	0.22 ± 0.03	3.72	6.13 ± 0.07
33	CH	2-Pyridinyl	CH_2-R^2	CMe_2-R^1	Me	>1000	2.07	<3.93
34	CH	2-Pyridinyl	CH_2-R^2	CH_2-R^1	^{i}Pr	>1000	2.64	<3.36
36		2-Pyridinyl	Me	Me	^{i}Pr	>1000	3.53	<2.47

[a] Mean ± SD for $n = 6$, except for **1** ($n = 60$).
[b] Binding data from reference 27.
[c] Measured value, $n = 6$.

(6.3) (Table 1). In addition, we had found that removal of the pendant phenyl group in the scaffold does not seriously affect binding affinity and that LipE was maintained as a result of a decrease in lipophilicity (clog*D*) by about 2 units [27]. Seeking to exploit the apparent benefit of reducing the size of this substituent and concomitantly molecular weight, we swapped the large and lipophilic pendant aryl group in **20** for the small and polar methoxy group (Table 1, **27**). This replacement conserved high LipE despite some decrease in TSPO affinity and established that TSPO is quite tolerant for such substitutions.

Tertiary amides are present in nearly all high-affinity TSPO ligands (e.g., see Chart 1). We sought further improvements to LipE by manipulation of substituents on the tertiary amido group. Previously, we also reported some TSPO ligands based on the scaffold in Chart 2 that incorporated a methylene tether to the amide in place of the oxygen tether [27]. As a group, these methylene-tethered ligands had lower LipE scores than the analogous oxygen-tethered ligands. Because LipE improved by about 1 unit when a phenylamide was exchanged for an isopropylamide in the methylene-tethered series [27], we expected a similar improvement in the oxygen-tethered series, and indeed this was found when comparing the new ligand **22** with **11** (Table 1).

Previously, we had found that the elimination of amide bond rotation in a methylene-tethered TSPO ligand, 1-methyl-3-[(2-phenylquinolin-4-yl)methyl]pyrrolidin-2-one (**30**), increased LipE by about 1 unit [27]. Therefore, we were interested to exploit this effect again by making a locked amide rotamer of ligand **22**. There are two possible ligands that may result from tethering the α-methyl group in **22** to one of its amide substituents, namely the ligands **33** and **34** (Table 1). Unlike the locked rotamer from our earlier study, both **33** and **34** showed no binding affinity for TSPO (Table 1). These results add to previous observations of locked amide rotamers showing much reduced affinity for TSPO [42]. Moreover, evidence indicates that TSPO has a preference to bind the *E*-rotamer of PK11195 (**1**) [43,44]. Thus, it seems that TSPO is highly sensitive to the spatial arrangement of the substituents on the requisite tertiary amide in TSPO ligands.

Finally, we tested a truncated scaffold analog of **11**. This ligand (Table 1, **36**) has a fused bicyclic scaffold whose structure is rather similar to that found in many literature TSPO ligands, as exemplified by DPA-713 (**4**), PBR111 (**7**) and IGA-1 (**37**) [45] (Chart 3). Ligand **36** appears to occupy essentially the same chemical space as these compounds, so we were surprised that **36** showed no binding to TSPO ($K_i > 1000$ nM). However, simple comparison of the formal 2-dimensional structure of **36** with those of other known TSPO ligands with similar core scaffolds shows that the amido carbonyl group, a key pharmacophoric element, is not aligned with the carbonyl groups of the other ligands. Hence, the inability of **36** to form a required directional hydrogen bond with TSPO may explain its lack of affinity.

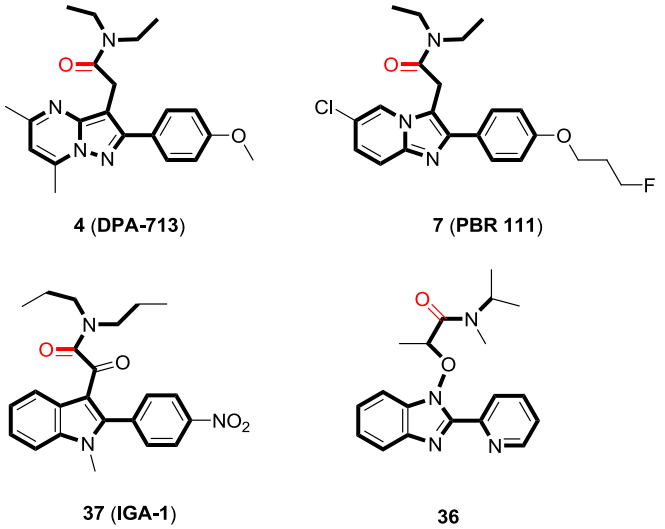

Chart 3. Comparison of formal structures of three high-affinity TSPO ligands with **36**. Bold bonds indicate scaffold matching that in ligand **4**. For ligands **4**, **7**, and **37**, a carbonyl group, shown in red, is part of the matching scaffold, but not for compound **36**. (For interpretation of the references to color in this figure legend, the reader is referred to the web version of this article.)

2.3. Pharmacological screen

Ligand **11**, at 10 μM concentration, showed <50% inhibition of specific binding to all tested receptors and transporters, except the 5-HT_{1A} receptor (K_i = 366 nM).

2.4. Radioligand syntheses

The radioligands [^{11}C]**11** and [^{11}C]**20** were produced in practically useful radiochemical yields in only 5 min at room temperature by treating their respective *N*-desmethyl precursors, **19** and **18**, with [^{11}C]methyl triflate [46] (Scheme 6). Each radioligand was separated with reversed phase HPLC and readily formulated in sterile ethanol with 10% saline, for possible use in PET scanning. Each radioligand was obtained with high radiochemical purity (>99%) and with high specific activities (244 and 126 GBq/μmol, respectively).

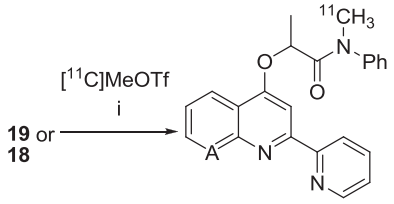

[^{11}C]**11**, A = CH
[^{11}C]**20**, A = N

Scheme 6. Radiosyntheses of [^{11}C]**11** and [^{11}C]**20**. Reagents and conditions: (i) for [^{11}C]**11**; NaOH, MeCN, rt, 5 min; for [^{11}C]**20**; NaH, MeCN, rt, 5 min.

2.5. Lipophilicity

The accessibility of [^{11}C]**11** and [^{11}C]**20** afforded the opportunity to measure their lipophilicities accurately for comparison to their computed values. Prolonged incubation of these radioligands in phosphate buffer (pH 7.4) at room temperature left them unchanged chemically. Although the measured log*D* for [^{11}C]**11** (3.11) was appreciably lower than the computed value (4.18), the measured log*D* of [^{11}C]**20** (2.48) was quite similar to the computed value (2.80) (Table 1). The computed values are therefore likely to be reasonable estimates (within one log unit of true values), and are also expected to be in approximately correct rank order for the closely related compounds. The measured values for both radioligands placed them near or within the desirable log*D* range of 2–4.

3. Conclusions

Modifications to *N*-methyl-(quinolin-4-yl)oxypropanamides, especially introduction of nitrogen into the 2-arylquinolin-4-yl scaffold, and use of an isopropyl substituent instead of a phenyl substituent on the tertiary amido nitrogen, were effective in retaining LipE to within a desirable range for PET radioligands. Cyclization of the amido group or contraction of the quinolinyl ring abolished high affinity. Three compounds (**20**–**22**) showed favorable properties for PET radioligand development, including high TSPO affinity and moderate computed lipophilicity. Ligands **11** and **20** were shown further to be amenable to labeling with carbon-11, to have acceptable moderate measured lipophilicity, and to be selective for binding to TSPO.

4. Experimental section

4.1. Materials and methods

Literature methods were used to prepare ligand **11** [27], 2-(pyridin-2-yl)-quinolin-4(1*H*)-one [30], 2-bromo-*N*-methyl-*N*-phenylpropanamide [47], 2-hydroxy-*N*-methyl-*N*-phenylpropanamide [48], 1,5,5-trimethylpyrrolidin-2-one [49], and 1-isopropylpyrrolidin-2-one [50]. All other reagents and solvents were purchased. Air-sensitive reagents were stored under N_2 in a PureLab HE glovebox (Innovative Technology; Amesbury, MA). Melting points were determined on an SMP30 apparatus (Stuart; Staffordshire, UK). Boiling point vacuum pressures were determined on a DDR-1200 apparatus (J-Kem Scientific Inc.; St. Louis, MO). Reactions in dry solvent were performed with dried reagents under an inert atmosphere. Solutions were taken to dryness by treatment with $MgSO_4$ (unless stated otherwise), followed by filtration and evaporation. ^{1}H (400 MHz), ^{13}C NMR (100 MHz), and ^{19}F NMR (376 MHz) spectra were recorded on an Avance 400 instrument (Bruker; Billerica, MA). Chemical shifts for ^{19}F are reported relative to neat TFA in a coaxial insert (δ = −76.6). HRMS data were obtained at the University of Illinois Urbana-Champaign (Mass Spectrometry Laboratory, School of Chemical Sciences) with a Micromass Q-Tof Ultima instrument for ESI (Waters; Milford, MA). Preparative HPLC was performed with elution at 30 mL/min on either a Luna PFP(2) column (5 μm; 100 Å; 30 × 250 mm; Phenomenex; Torrance, CA), or a Gemini C18 column (10 μm; 110 Å; 30 × 250 mm; Phenomenex). Compound purities were established on either a Luna PFP(2) column (5 μm; 100 Å; 4.6 × 250 mm; Phenomenex) or a Gemini C18 column (5 μm; 110 Å; 4.6 × 250 mm; Phenomenex). All compounds were >95% pure and typically >99% pure, as monitored by absorbance at 220 nm. Radioligands were isolated with HPLC on an XBridge C_{18} column (5 μm; 130 Å; 10 × 250 mm; Waters) or a Luna C18(2) column (10 μm; 100 Å; 10 × 250 mm; Phenomenex). Radiochemical purities were determined with HPLC on an XTerra RP_{18} column (10 μm, 125 Å, 7.8 × 300 mm; Waters) using a Gold HPLC apparatus (Beckman Coulter, Inc.; Fullerton, CA) equipped with an in-line Flow-Count NaI scintillation detector (Bioscan, Inc.; Washington, DC) and a UV absorbance detector (Beckman Coulter, Inc.) operating at 254 nm. Radioactive decay events were counted in an automatic gamma counter (1480 Wizard 3; PerkinElmer Life Sciences: Wallac Oy; Turku, Finland) with an electronic window set between 360 and 1800 keV. c*LogD* values were computed with Pallas for Windows software version 3.8 in default option (CompuDrug; Bal Harbor, FL).

4.2. Chemistry

4.2.1. *N*-(3-Acetylpyridin-2-yl)picolinamide (**12**)

Pyridine-2-carbonyl chloride hydrochloride (4.89 g, 27.5 mmol) was added portion-wise to a solution of 1-(2-amino-3-pyridinyl)-1-ethanone (5.15 g, 37.8 mmol) and TEA (9.2 mL, 65.0 mmol) in dry $CHCl_3$ (100 mL) at 4 °C. The mixture turned from tan to deep blue-green and the temperature rose to 15 °C. After 29 h, the mixture was diluted with $CHCl_3$ (100 mL) and washed with hydrochloric acid (1 M; 100 mL × 2), water (100 mL), and brine (100 mL × 2), and then dried. The product was recrystallized (MTBE–$CHCl_3$) to give a tan powder (714 mg, 11%). A second recrystallization (MTBE–MeOH) gave **12** as a cream-white powder. mp 151–154 °C. HRMS-ESI (*m*/*z*): $[M+H]^+$ calcd for $C_{13}H_{12}N_3O_2$, 242.0930; found, 242.0929. ^{1}H NMR ($CDCl_3$): δ 13.22 (bs, 1H), 8.79 (dq, *J* = 4.8, 0.8 Hz, 1H), 8.74 (dd, *J* = 4.8, 2.0 Hz, 1H), 8.35 (td, *J* = 8.0, 1.2 Hz, 1H), 8.24 (dd, *J* = 8.0, 2.0 Hz, 1H), 7.91 (dt, *J* = 8.0, 2.0 Hz, 1H), 7.51 (ddd, *J* = 7.6, 4.8, 1.2 Hz, 1H), 7.18 (dd, *J* = 7.6, 4.8 Hz, 1H), 2.71 (s, 3H). ^{13}C NMR ($CDCl_3$): δ 200.2, 162.6, 153.2, 151.1, 150.1, 148.5, 139.8, 137.5,

126.7, 123.2, 119.3, 118.5, 28.0.

4.2.2. N-(2-Acetylphenyl)pyrimidine-2-carboxamide (**13**)

DMF (30 mL) was added dropwise to a slurry of sodium pyrimidine-2-carboxylate (5.03 g, 34.4 mmol), 2′-aminoacetophenone (4.6 mL, 37 mmol), DIPEA (6.5 mL, 37 mmol) and PyBroP (17.4 g, 37.4 mmol) in CH_2Cl_2 (40 mL) held in a water bath, wherein the temperature rose from 21 to 29 °C. As the colorless slurry dissolved, the solution turned from orange to a deep forest green over the course of 18 h. The solvent was removed. The residue was taken up in EtOAc (370 mL), then washed successively with aq $KHSO_4$ (5% w/v, 370 mL × 3), brine (370 mL), aq $NaHCO_3$ (5% w/v, 370 mL × 3), brine (370 mL), and dried (Na_2SO_4). The residue was washed with ether and dioxane and recrystallized (MTBE–$CHCl_3$; charcoal to decolorize) to give **13** as golden-yellow plates (435 mg, 5%). mp 201–203 °C. HRMS-ESI (*m*/*z*): $[M+H]^+$ calcd for $C_{13}H_{12}N_3O_2$, 242.0930; found, 242.0928. ^{1}H NMR ($CDCl_3$): δ 13.65 (bs, 1H), 9.09 (dd, *J* = 8.4, 0.8 Hz, 1H), 9.03 (d, *J* = 5.2 Hz, 2H), 7.98 (dd, *J* = 8.0, 1.6 Hz, 1H), 7.66 (ddd, *J* = 8.4, 7.6, 1.2 Hz, 1H), 7.50 (t, *J* = 4.8 Hz, 1H), 7.22 (ddd, *J* = 8.4, 7.6, 1.2 Hz, 1H), 2.74 (s, 3H). ^{13}C NMR ($CDCl_3$): δ 202.4, 161.3, 158.2, 157.8, 139.9, 135.1, 131.7, 123.2, 122.9, 122.6, 121.2, 28.6.

4.2.3. 2-(Pyridin-2-yl)-1,8-naphthyridin-4(1H)-one (**14**)

Compound **12** (716 mg, 2.97 mmol) and NaOH (355 mg, 8.88 mmol) in dry dioxane (40 mL) were heated to 95 °C for 3 h, whereupon the tan solution precipitated a brown solid. The mixture was cooled to rt, and the solid filtered off, washed with toluene (10 mL × 3), and taken up in H_2O (20 mL). The blood-red solution was neutralized with hydrochloric acid (1 M, ~7 mL) to precipitate a tan solid, which was filtered off, washed with water (10 mL × 2) followed by ether (10 mL × 2), and then recrystallized (toluene) to give **14** as a pink-tan solid with a cotton candy texture (165 mg). More **14** (60 mg) was obtained from the mother liquor (225 mg total, 34%). mp 205–206 °C. HRMS-ESI (*m*/*z*): $[M+H]^+$ calcd for $C_{13}H_{10}N_3O$, 224.0824; found, 224.0829. ^{1}H NMR ($CDCl_3$): δ 10.78 (bs, 1H), 8.76 (td, *J* = 2.8, 1.2 Hz, 1H), 8.74 (dd, *J* = 4.4, 1.6 Hz, 1H), 8.68 (dd, *J* = 7.6, 1.6 Hz, 1H), 8.01 (td, *J* = 7.2, 0.8 Hz, 1H), 7.92 (dt, *J* = 7.6, 1.6 Hz, 1H), 7.47 (ddd, *J* = 7.2, 4.8, 0.8 Hz, 1H), 7.35 (dd, *J* = 8.0, 3.6 Hz, 1H), 7.00 (br s, 1H). ^{13}C NMR ($CDCl_3$): δ 179.8, 153.6, 150.1, 149.3, 148.2, 145.6, 137.7, 135.5, 125.5, 120.9, 120.5, 120.0, 107.2.

4.2.4. 2-(Pyrimidin-2-yl)quinolin-4(1H)-one (**15**)

Compound **13** (407 mg, 1.69 mmol) and NaOH (202 mg, 5.05 mmol) in dry dioxane (15 mL) were heated in a pressure vessel to 110 °C for 3 h, during which time the pale yellow solution turned yellow-brown and a red-orange solid precipitated. After cooling the mixture to rt, the solid was filtered off, washed with dioxane, taken up in water (20 mL), and brought to pH 5 with acetic acid, whereupon the orange solution gave a salmon-pink precipitate. The solid was filtered off, washed with water, and recrystallized (toluene) to give **15** as a light pink solid (187 mg, 50%). mp 258 °C (dec). HRMS-ESI (*m*/*z*): $[M+H]^+$ calcd for $C_{13}H_{10}N_3O$, 224.0824; found, 224.0827. ^{1}H NMR (DMSO-d_6, *keto*–*enol*; 1.4:1.0): δ 12.14 (bs, 1H, *keto*), 9.10 (d, *J* = 4.8 Hz, 2H, *keto* + *enol*), 8.12 (d, *J* = 8.8 Hz, 2H, *keto* + *enol*), 7.74–7.68 (m, 2H, *keto* + *enol*), 7.37 (dt, *J* = 6.8, 0.8 Hz, 1H, *keto* + *enol*), 7.15 (s, 1H, *keto* + *enol*), 3.34 (s, 1H, *enol*). ^{13}C NMR (DMSO-d_6): δ 177.7 (*keto*), 158.3 (*enol*), 158.0 (*keto*), 144.7 (*enol*), 144.6, 140.3 (*enol*), 140.2 (*keto* + *enol*), 132.2 (*keto* + *enol*), 125.8 (*keto* + *enol*), 124.7 (*keto* + *enol*), 123.6 (*keto* + *enol*), 122.3 (*keto* + *enol*), 119.6 (*keto* + *enol*), 108.0 (*keto* + *enol*).

4.2.5. 2-Bromo-N-isopropyl-N-methylpropanamide (**16**)

N-Isopropylmethylamine (1.0 mL, 9.8 mmol) was added to a biphasic solution of KOH (1.67 g, 29.7 mmol) in water (10 mL) and EtOAc (10 mL). This mixture was stirred rapidly and cooled to 4 °C whereupon 2-bromopropanoyl chloride (1.5 mL, 15 mmol) was added dropwise with the temperature kept below 11 °C. The ice bath was removed and stirring continued for 1.5 h. The organic phase was separated off and the aqueous phase extracted with EtOAc (5 mL × 2). The combined extracts were washed with brine (10 mL) and dried. The residue was distilled (bp 48–50 °C at 0.2 mmHg), but was still contaminated with 2-bromopropanoic acid. The oil was taken up in $CHCl_3$ (10 mL), washed with NH_4OH (5 mL × 3), water (5 mL), and brine (5 mL × 2), and then dried to give **16** as a colorless oil (588 mg, 29%). *d* 1.38 g/mL. HRMS-ESI (*m*/*z*): $[M+H]^+$ calcd for $C_7H_{15}BrNO$, 208.0337; found, 208.0341. ^{1}H NMR ($CDCl_3$, *cis*–*trans*; 1.4:1.0): δ 4.84 (sept, *J* = 6.8 Hz, 1H, *cis*), 4.60 (q, *J* = 6.4 Hz, 1H, *trans*), 4.53 (q, *J* = 6.4 Hz, 1H, *cis*), 4.20 (sept, *J* = 6.8 Hz, 1H, *trans*), 2.91 (s, 3H, *cis*), 2.81 (s, 3H, *trans*), 1.84 (d, *J* = 5.6 Hz, 3H, *trans*), 1.83 (d, *J* = 6.4 Hz, 3H, *trans*), 1.27 (d, *J* = 6.8 Hz, 3H, *trans*), 1.21 (d, *J* = 6.8 Hz, 3H, *cis*), 1.12 (d, *J* = 7.2 Hz, 3H, *cis*), 1.10 (d, *J* = 6.8 Hz, 3H, *cis*). ^{13}C NMR ($CDCl_3$): δ 168.6 (*cis*), 168.4 (*trans*), 48.3 (*trans*), 44.8 (*trans*), 39.5 (*cis*), 38.5 (*trans*), 28.3 (*cis*), 26.6 (*trans*), 22.1 (*trans*), 21.7 (*cis*), 20.8 (*trans*), 19.9 (*trans*), 19.4 (*cis*), 18.8 (*cis*).

4.2.6. 2-Bromo-N-(4-fluorophenyl)-N-methylpropanamide (**17**)

The method for **16** was applied to 4-fluoro-*N*-methylaniline (3.5 mL, 29 mmol) and 2-bromopropanoyl chloride (4.4 mL, 44 mmol). The crude product oil was fractionally distilled. The forerun (bp 37–39 °C at 7.2 mmHg; 0.2 mL) was discarded and **17** (6.7 g, 88%) was collected as a yellow oil (bp 84–88 °C at 5.7 mmHg; *d* 1.5 g/mL). HRMS-ESI (*m*/*z*): $[M+H]^+$ calcd for $C_{10}H_{12}BrFNO$, 260.0086; found, 260.0090. ^{1}H NMR ($CDCl_3$): δ 7.29 (m, 2H), 7.14 (m, 2H), 4.22 (q, *J* = 6.8 Hz, 1H), 3.28 (s, 3H), 1.74 (d, *J* = 6.4 Hz, 3H). ^{13}C NMR ($CDCl_3$): δ 169.6, 162.1 (d, *J* = 247 Hz), 138.8 (d, *J* = 3 Hz), 129.1 (d, *J* = 9 Hz), 116.9 (d, *J* = 22 Hz), 38.8, 38.2, 21.7. ^{19}F NMR ($CDCl_3$): δ −113.0.

4.2.7. N-Phenyl-2-[2-(pyridin-2-yl)-1,8-naphthyridin-4-yloxy] propanamide (**18**)

NaH (20 mg, 0.50 mmol; 60% in mineral oil) was added to a solution of **14** (60 mg, 0.27 mmol) in dry DMSO (2 mL). The orange effervescent solution was stirred for 1 h, whereupon 2-bromo-*N*-phenylpropanamide (192 mg, 0.84 mmol) was added. The mixture was heated to 80 °C for 8 h, cooled to rt and quenched with water (15 mL). The precipitate was filtered off, washed with water and purified with HPLC [PFP column; MeOH–$NH_4CH_3CO_2$ buffer (25 mM, pH 5); 70:30] to give a peach solid (14 mg, 14%), which was recrystallized (toluene–MTBE) to give **18**. mp 222–223 °C. HRMS-ESI (*m*/*z*): $[M+H]^+$ calcd for $C_{22}H_{19}N_4O_2$, 371.1508; found, 371.1503. ^{1}H NMR ($CDCl_3$): δ 9.13 (dd, *J* = 4.0, 2.0 Hz, 1H), 8.75 (d, *J* = 8.0 Hz, 1H), 8.74 (ddd, *J* = 4.8, 2.8, 0.8 Hz, 1H), 8.57 (dd, *J* = 8.4, 2.0 Hz, 1H), 8.44 (bs, 1H), 8.20 (s, 1H), 7.82 (dt, *J* = 7.6, 1.6 Hz, 1H), 7.61 (dd, *J* = 8.8, 1.2 Hz, 2H), 7.46 (dd, *J* = 8.4, 4.4 Hz, 1H), 7.38–7.31 (3H), 7.14 (tt, *J* = 7.6, 0.8 Hz, 1H), 5.37 (q, *J* = 6.8 Hz, 1H), 1.85 (d, *J* = 6.8 Hz, 3H). ^{13}C NMR ($CDCl_3$): δ 168.4, 160.5, 160.5, 157.0, 154.8, 154.0, 149.0, 137.0, 136.9, 131.2, 129.1, 125.0, 124.9, 122.4, 121.5, 120.4, 116.1, 100.2, 75.7, 18.2.

4.2.8. N-Phenyl-2-[2-(pyridin-2-yl)quinolin-4-yloxy]propanamide (**19**)

2-(Pyridin-2-yl)quinolin-4(1*H*)-one (222 mg, 1.00 mmol), 2-bromo-*N*-phenylpropanamide (255 mg, 1.12 mmol), and K_2CO_3 (834 mg, 6.03 mmol) in MeCN (35 mL) were heated to 55 °C for 8 h. The mixture was cooled to rt and poured into water (175 mL). The precipitate was filtered off and recrystallized (aq dioxane) to give **19** as a colorless powder (283 mg, 77%). mp 205–206 °C. ^{1}H NMR

($CDCl_3$): δ 8.70 (qd, J = 4.8, 0.8 Hz, 1H), 8.63 (md, J = 9.2, 0.8 Hz, 1H), 8.29 (dd, J = 8.4, 0.8 Hz, 1H), 8.22 (bs, 1H), 8.17 (d, J = 8.4 Hz, 1H), 8.13 (s, 1H), 7.85 (dt, J = 8.0, 2.0 Hz, 1H), 7.80 (ddd, J = 7.2, 5.6, 0.6 Hz, 1H), 7.61 (ddd, J = 8.4, 6.8, 0.6 Hz, 1H), 7.55–7.52 (2H), 7.35 (ddd, J = 7.6, 4.8, 1.2 Hz, 1H), 7.34–7.29 (2H), 7.12 (m, 1H), 5.40 (q, J = 6.8 Hz, 1H), 1.87 (d, J = 6.8 Hz, 3H). ^{13}C NMR ($CDCl_3$): δ 168.9, 159.9, 157.6, 155.7, 149.3, 149.1, 136.9, 136.9, 130.3, 129.8, 129.1, 126.5, 124.9, 124.3, 121.7, 121.2, 121.2, 120.2, 99.6, 75.2, 18.4.

4.2.9. *N*-Methyl-*N*-phenyl-2-[2-(pyridin-2-yl)-1,8-naphthyridin-4-yloxy]propanamide (**20**)

2-Bromo-*N*-methyl-*N*-phenylpropanamide (122 mg, 0.50 mmol), **14** (100 mg, 0.45 mmol), and K_2CO_3 (371 mg, 2.69 mmol) in dry MeCN (10 mL) were heated to 55 °C for 18 h. The mixture was cooled to rt and filtered through diatomaceous earth. The solvent was removed, the residue taken up in CH_2Cl_2 (10 mL), extracted into hydrochloric acid (2 M; 30 mL × 2), and neutralized with satd. $NaHCO_3$. The solution was extracted with CH_2Cl_2 (50 mL × 3) and the combined organic layers washed with water (50 mL) and brine (50 mL × 2), and then dried. The product was isolated by HPLC [PFP column; MeOH–phosphate buffer (25 mM, pH 6); 80:20] followed by recrystallization (cyclohexane–dioxane) to give **20** as a cream solid (17 mg, 10%). mp 193–194 °C. HRMS-ESI (m/z): $[M+H]^+$ calcd for $C_{23}H_{21}N_4O_2$, 385.1665; found, 385.1664. ^{1}H NMR ($CDCl_3$): δ 9.08 (dd, J = 4.4, 2.4 Hz, 1H), 8.90 (d, J = 8.0 Hz, 1H), 8.78 (d, J = 4.0 Hz, 1H), 8.66 (dd, J = 8.0, 2.0 Hz, 1H), 8.03 (s, 1H), 7.89 (dt, J = 8.0, 2.0 Hz, 1H), 7.68 (bs, 2H), 7.50 (t, J = 7.6 Hz, 2H), 7.45–7.38 (3H), 5.08 (q, J = 6.4 Hz, 1H), 3.33 (s, 3H), 1.69 (d, J = 6.4 Hz, 3H). ^{13}C NMR ($CDCl_3$): δ 169.9, 161.4, 159.9, 157.0, 155.5, 153.7, 148.6, 142.5, 137.0, 132.3, 130.3, 128.8, 127.8, 124.7, 122.5121.0, 116.3, 99.7, 71.7, 50.7, 38.1, 18.4.

4.2.10. *N*-Methyl-*N*-phenyl-2-[2-(pyrimidin-2-yl)quinolin-4-yl]oxypropanamide (**21**)

2-Bromo-*N*-methyl-*N*-phenylpropanamide (216 mg, 0.89 mmol), **15** (179 mg, 0.80 mmol), and K_2CO_3 (1.04 g, 7.53 mmol) in dry MeCN (10 mL) were heated to 55 °C for 4.5 h, whereupon the colorless slurry turned yellow. The mixture was cooled to rt and filtered through diatomaceous earth. The solvent was removed and the residue taken up in CH_2Cl_2 (100 mL), washed with water (50 mL × 2) followed by brine (50 mL), dried, and recrystallized (cyclohexane–dioxane) to give **21** as a colorless solid (263 mg, 86%). mp 211–212 °C. HRMS-ESI (m/z): $[M+H]^+$ calcd for $C_{23}H_{21}N_4O_2$, 385.1665; found, 385.1665. ^{1}H NMR ($CDCl_3$): δ 9.02 (d, J = 4.8 Hz, 2H), 8.32 (d, J = 8.4 Hz, 1H), 8.26 (d, J = 8.4 Hz, 1H), 7.87 (s, 1H), 7.72 (dt, J = 6.8, 1.2 Hz, 1H), 7.55–7.51 (3H), 7.41–7.37 (3H), 7.32 (t, J = 7.2 Hz, 1H), 5.09 (q, J = 6.8 Hz, 1H), 3.34 (s, 3H), 1.69 (d, J = 6.4 Hz, 3H). ^{13}C NMR ($CDCl_3$): δ 170.0, 163.7, 161.0, 157.6, 155.3, 149.4, 142.6, 130.2, 130.1, 130.0, 128.6, 127.7, 126.6, 122.1, 121.7, 120.6, 100.6, 71.5, 38.2, 18.3.

4.2.11. *N*-Isopropyl-*N*-methyl-2-[2-(pyridin-2-yl)quinolin-4-yloxy]propanamide (**22**)

The method for **21** was applied to 2-(pyridin-2-yl)-quinolin-4(1*H*)-one (222 mg, 1.00 mmol) and **16** (170 μL, 1.12 mmol). The crude product was recrystallized (aq EtOH) to give **22** as white sea urchin-shaped clusters (219 mg, 63%). mp 175–176 °C. HRMS-ESI (m/z): $[M+H]^+$ calcd for $C_{21}H_{24}N_3O_2$, 350.1869; found, 350.1868. ^{1}H NMR ($CDCl_3$, *cis*–*trans*; 1.1:1.0): δ 8.67–8.64 (4H, *cis* + *trans*), 8.31 (d, J = 8.4 Hz, 2H, *cis* + *trans*), 8.10 (d, J = 8.4 Hz, 2H, *cis* + *trans*), 7.95 (s, 1H, *trans*), 7.90 (s, 1H, *cis*), 7.85 (tt, J = 7.6, 2.0 Hz, 2H, *cis* + *trans*), 7.72 (dd, J = 6.8, 1.6 Hz, 1H, *cis*), 7.71 (dd, J = 6.8, 1.6 Hz, 1H, *trans*), 7.53 (dd, J = 6.8, 1.2 Hz, 1H, *cis*), 7.51 (dd, J = 6.8, 1.2 Hz, 1H, *trans*), 7.35–7.31 (2H, *cis* + *trans*), 5.55 (q, J = 6.8 Hz, 1H, *trans*), 5.41 (q, J = 6.4 Hz, 1H, *cis*), 4.91 (sept, J = 6.8 Hz, 1H, *cis*), 4.35 (sept, J = 6.4 Hz, 1H, *trans*), 3.02 (s, 3H, *cis*), 2.84 (s, 3H, *trans*), 1.78 (d, J = 6.4 Hz, 3H, *trans*), 1.77 (d, J = 6.8 Hz, 3H, *cis*), 1.38 (d, J = 6.4 Hz, 3H, *trans*), 1.17 (d, J = 6.4 Hz, 3H, *trans*), 1.16 (d, J = 6.8 Hz, 3H, *cis*), 1.10 (d, J = 6.8 Hz, 3H, *cis*). ^{13}C NMR ($CDCl_3$): δ 169.4 (*cis*), 169.2 (*trans*), 160.8 (*cis*), 160.7 (*trans*), 157.3 (*trans*), 157.2 (*cis*), 156.2 (*trans*), 156.1 (*cis*), 149.2 (*cis* + *trans*), 148.9 (*cis* + *trans*), 136.8 (*cis* + *trans*), 129.9 (*cis*), 129.3 (*trans*), 125.9 (*cis* + *trans*), 124.1 (*cis* + *trans*), 122.1 (*cis* + *trans*), 121.7 (*trans*), 121.6 (*cis*), 121.3 (*cis* + *trans*), 98.7 (*cis*), 98.6 (*trans*), 72.3 (*cis*), 72.1 (*trans*), 47.7 (*trans*), 44.8 (*cis*), 39.5 (*cis*), 38.5 (*trans*), 28.3 (*cis*), 26.6 (*trans*), 22.1 (*trans*), 21.7 (*cis*), 20.8 (*trans*), 19.9 (*trans*), 19.4 (*cis*), 18.8 (*cis*).

4.2.12. *N*-(4-Fluorophenyl)-*N*-methyl-2-[2-(pyridin-2-yl)quinolin-4-yloxy]propanamide (**23**)

The method for **21** was applied to 2-(pyridin-2-yl)-quinolin-4(1*H*)-one (222 mg, 1.00 mmol) and **17** (195 μL, 1.12 mmol). The crude product was recrystallized (aq dioxane) to give white crystals. These were dried in an Abderhalden pistol under high vacuum (T = 110 °C) in the presence of P_2O_5 for 1 d to give **23** (293 mg, 73%). mp 179–180 °C. HRMS-ESI (m/z): $[M+H]^+$ calcd for $C_{24}H_{21}FN_3O_2$, 402.1618; found, 402.1613. ^{1}H NMR ($CDCl_3$): δ 8.75 (d, J = 4.0 Hz, 1H), 8.70 (d, J = 8.0 Hz, 1H), 8.27 (dd, J = 8.4, 0.8 Hz, 1H), 8.08 (d, J = 8.0 Hz, 1H), 7.88 (dt, J = 7.6, 1.6 Hz, 1H), 7.82 (s, 1H), 7.70 (dt, J = 8.0, 1.2 Hz, 1H), 7.68 (br s, 2H), 7.50 (dt, J = 8.0, 0.8 Hz, 1H), 7.38 (ddd, J = 7.6, 4.8, 1.2 Hz, 1H), 7.15 (dt, J = 8.0, 1.2 Hz, 2H), 5.04 (q, J = 6.4 Hz, 1H), 3.31 (s, 3H), 1.87 (d, J = 6.4 Hz, 3H). ^{13}C NMR ($CDCl_3$): δ 170.3, 162.3 (d, J = 248 Hz), 160.7, 156.9, 156.2, 149.2, 148.6, 138.6 (d, J = 3 Hz), 137.0, 130.0, 129.8 (d, J = 8 Hz), 129.1, 125.9, 124.2, 122.3, 121.8, 121.3, 117.2 (d, J = 22 Hz), 98.6, 71.1, 38.3, 18.5. ^{19}F NMR ($CDCl_3$): δ − 112.9.

4.2.13. Methyl 2-(1-methoxyethylideneamino)nicotinate (**24**)

Methyl 2-aminopyridine-3-carboxylate (5.17 g, 34.0 mmol) was heated to 110 °C for 1 h in a mixture of trimethyl orthoacetate (50 mL) and acetic anhydride (20 mL), whereupon the colorless solution turned yellow. After 1 h, methyl acetate began to distill off and heating was continued for 5 h. The excess reagents were removed in vacuo leaving a red oil and white syrup. This was taken up in Et_2O (100 mL) and washed with aq Na_2CO_3 (2 M, 50 mL × 2), water (50 mL), and brine (50 mL × 2), and then dried. The residue was purified by Kugelrohr distillation (140–160 °C at 1.3 mmHg) to yield **24** as a yellow oil which smelled like sugar snap peas (2.00 g, 28%). HRMS-ESI (m/z): $[M+H]^+$ calcd for $C_{10}H_{13}N_2O_3$, 209.0926; found, 209.0930. ^{1}H NMR ($CDCl_3$): δ 8.51 (dd, J = 4.8, 1.6 Hz, 1H), 8.21 (dd, J = 7.6, 2.0 Hz, 1H), 7.06 (dd, J = 8.0, 4.8 Hz, 1H), 3.87 (s, 3H), 3.86 (s, 3H), 1.87 (s, 3H). ^{13}C NMR ($CDCl_3$): δ 165.9, 163.1, 160.7, 152.3, 140.0, 118.3, 117.6, 53.9, 52.1, 17.2.

4.2.14. 2-Methoxy-1,8-naphthyridin-4(1H)-one (**25**)

A solution of **24** (1.9 g, 9.1 mmol) in dry THF (10 mL) was added dropwise to a slurry of LDA (10 mmol) in THF–hexane (10 mL) at −50 °C, whereupon the solution turned bright orange. After 1 h, the temperature was raised to 0 °C. The solution was stirred for another 30 min and quenched with cold satd. NH_4Cl (25 mL) followed by aq Na_2CO_3 (2 M, 50 mL). The aqueous layer was separated off, washed with Et_2O (50 mL × 2), and carefully neutralized with hydrochloric acid (1 M) to give a white precipitate. Product remaining in the mother liquor was extracted into BuOH (50 mL × 4), which was washed with brine (50 mL × 2), and dried. The product was isolated with HPLC [PFP column; MeOH–NH_4HCO_2 buffer (25 mM, pH 4); 35:65] to give **25** as a cream solid (1.2 g, 76%). mp ~160 °C (dec; if ramping was omitted: ~200 °C dec). HRMS-ESI (m/z): $[M+H]^+$ calcd for $C_9H_9N_2O_2$, 177.0664; found, 177.0665. ^{1}H NMR (HFIP-d_2): δ 8.82 (dd, J = 8.0, 1.2 Hz, 1H), 8.64 (dd, J = 4.8, 1.6 Hz, 1H), 7.57 (dd, J = 8.0, 5.2 Hz, 1H),

6.27 (s, 1H), 4.11 (s, 3H). ^{13}C NMR (HFIP-d_2): δ 164.2, 149.9, 146.8, 136.9, 119.5, 116.7, 90.6, 55.3.

4.2.15. 4-Chloro-2-methoxy-1,8-naphthyridine (**26**)

Method A: A slurry of 2,4-dichloro-1,8-naphthyridine (4.95 g, 24.9 mmol) in dry toluene (50 mL) was added to a slurry of NaOMe (5.0 g, 93 mmol) in toluene (50 mL) at rt. The temperature rose to 32 °C as the yellow solid dissolved to give a brown solution [Note-NaOMe should be broken up periodically if needed]. After 17 h, the mixture was filtered through diatomaceous earth, and washed with toluene. The solvent was removed and the residue recrystallized (aq EtOH) to give **26** as fine, light yellow needles (3.87 g). Concentration of the mother liquor yielded more product (250 mg; 4.12 g total, 85%). mp 134–135 °C. HRMS-ESI (*m*/*z*): $[M+H]^+$ calcd for $C_9H_8ClN_2O$, 195.0325; found, 195.0327. ^{1}H NMR ($CDCl_3$): δ 8.99 (dd, J = 4.4, 2.0 Hz, 1H), 8.48 (dd, J = 8.0, 2.0 Hz, 1H), 7.45 (dd, J = 8.0, 4.4 Hz, 1H), 7.12 (s, 1H), 4.16 (s, 3H). ^{13}C NMR ($CDCl_3$): δ 164.5, 155.4, 153.6, 143.7, 133.6, 120.5, 118.2, 114.0, 54.5. *Method B*: Compound **25** (1.20 g, 6.82 mmol) in $POCl_3$ (10 mL) was heated to 110 °C for 19 h to give an orange solution. The solution was cooled and carefully quenched by slow addition to water (100 mL) and neutralized with NH_4OH. This product was extracted into $CHCl_3$ (100 mL), washed with water (100 mL) followed by brine (100 mL × 2), and then dried. The product was isolated by HPLC [Gemini column; MeOH–NH_4HCO_2 buffer (25 mM, pH 7); 65:35] to give **26** as a pale yellow solid (41 mg, 3%). mp 132–133 °C.

4.2.16. 2-(2-Methoxy-1,8-naphthyridin-4-yloxy)-N-methyl-N-phenylpropanamide (**27**)

2-Hydroxy-*N*-methyl-*N*-phenylpropanamide (197 mg, 1.10 mmol) and NaH (44 mg, 1.10 mmol; 60%) were stirred in dry DMF (1.0 mL) at rt for 4 h. The red solution was transferred via cannula into a mixture of **26** (195 mg, 1.00 mmol) in DMSO–DMF (1:1; 2.0 mL). The reaction stalled after 30 min so the product was isolated with HPLC [PFP column; MeOH–NH_4HCO_2 buffer (25 mM, pH 7); 75:25, followed by Gemini column; MeOH–NH_4HCO_2 buffer (25 mM, pH 7); 70:30] to yield **27** as small, colorless needles (112 mg, 33%). mp 151–152 °C. HRMS-ESI (*m*/*z*): $[M+H]^+$ calcd for $C_{19}H_{20}N_3O_3$, 338.1505; found, 338.1499. ^{1}H NMR ($CDCl_3$): δ 8.88 (dd, J = 4.4, 2.0 Hz, 1H), 8.39 (dd, J = 8.4, 2.0 Hz, 1H), 7.43–7.34 (3H), 7.28–7.25 (3H), 5.94 (s, 1H), 4.88 (q, J = 6.8 Hz, 1H), 4.11 (s, 3H), 3.33 (s, 3H), 1.61 (d, J = 6.8 Hz, 3H). ^{13}C NMR ($CDCl_3$): δ 169.3, 165.9, 161.5, 156.0, 152.9, 142.3, 132.0, 130.2, 128.7, 127.2, 119.0, 113.8, 92.5, 71.9, 54.1, 38.2, 17.9.

4.2.17. 2-(2-Aminoquinolin-4-yloxy)-N-methyl-N-phenylpropanamide (**28**)

2-Amino-4-hydroxyquinoline hydrate was dried in an Abderhalden pistol under high vacuum (T = 110 °C) in the presence of P_2O_5. A slurry of this quinoline (3.70 g, 23.1 mmol) with sodium ethoxide (24 mmol) in ethanol (9.1 mL) was heated to 70 °C, whereupon a red solution formed. The solvent was distilled off, leaving a white solid, which was dried under vacuum until the internal temperature returned to 70 °C. Dry DMF (20 mL) was added to the solid and the slurry heated to 90 °C. 2-Bromo-*N*-methyl-*N*-phenylpropanamide (5.87 g, 24.3 mmol) was added in one portion. Heating was continued for 30 min, whereupon NaBr gradually precipitated. The mixture was cooled to rt, poured into water (200 mL), and extracted into CH_2Cl_2 (150 mL × 3). The organic extracts were washed with water (40 mL × 5), brine (250 mL × 2), and finally dried (K_2CO_3). Recrystallization (aq EtOH) of the white solid gave light yellow crystals, which were dried in an Abderhalden pistol under high vacuum (T = 110 °C) in the presence of P_2O_5 to give **28** (4.50 g, 61%). mp 182–184 °C. HRMS-ESI (*m*/*z*): $[M+H]^+$ calcd for $C_{19}H_{20}N_3O_2$, 322.1556; found, 322.1552. ^{1}H NMR ($CDCl_3$): δ 7.83 (d, J = 8.0 Hz, 1H), 7.54 (q, J = 8.0 Hz, 1H), 7.54 (s, 1H), 7.30–7.28 (3H), 7.19–7.14 (3H), 5.67 (s, 1H), 4.90 (q, J = 6.4 Hz, 1H), 4.67 (s, 2H), 3.31 (s, 3H), 1.60 (d, J = 6.4 Hz, 3H). ^{13}C NMR ($CDCl_3$): δ 169.7, 161.0, 158.0, 148.6, 142.4, 130.2, 129.9, 128.4, 127.2, 125.3, 122.3, 121.9, 117.7, 90.5, 71.9, 38.4, 17.8.

4.2.18. 2-[2-(1H-Pyrrol-1-yl)quinolin-4-yloxy]-N-methyl-N-phenylpropanamide (**29**)

2,5-Dimethoxytetrahydrofuran (195 μL, 1.50 mmol) was added to a pale yellow solution of **28** (321 mg, 1.00 mmol) in acetic acid (4 mL) at 120 °C (bath temp.), causing the solution to turn red. This solution was heated for 25 min, cooled to rt, poured into CH_2Cl_2 (100 mL), and washed with NH_4OH (50 mL × 2), water (50 mL), and brine (50 mL × 2), and finally dried. The product was isolated with HPLC [PFP column; MeCN–$NH_4CH_3CO_2$ buffer (25 mM, pH 7); 70:30] to give **29** as a pale pink solid (90 mg, 24%). mp 130 °C (dec). HRMS-ESI (*m*/*z*): $[M+H]^+$ calcd for $C_{23}H_{22}N_3O_2$, 372.1712; found, 372.1713. ^{1}H NMR ($CDCl_3$): δ 8.07 (dd, J = 8.0, 0.4 Hz, 1H), 7.88 (d, J = 8.4 Hz, 1H), 7.88 (ddd, J = 8.4, 7.2, 1.6 Hz, 1H), 7.52 (d, J = 4.4 Hz, 1H), 7.52 (s, 1H), 7.40 (ddd, J = 8.0, 6.8, 1.2 Hz, 1H), 7.37–7.31 (3H), 7.23–7.21 (2H), 6.41 (s, 1H), 6.40 (t, J = 2.0 Hz, 2H), 5.04 (q, J = 6.4 Hz, 1H), 3.32 (s, 3H), 1.67 (d, J = 6.4 Hz, 3H). ^{13}C NMR ($CDCl_3$): δ 169.4, 161.9, 150.7, 148.0, 142.3, 130.7, 130.2, 128.7, 127.9, 127.3, 124.7, 122.4, 120.0, 118.6, 111.4, 91.8, 71.8, 38.3, 18.1.

4.2.19. 3-Chloro-1,5,5-trimethylpyrrolidin-2-one (**31**)

t-Butyl lithium (1.64 M; 17 mmol) in pentane (2.3 mL) was added dropwise to a solution of 2-bromomesitylene (fractionally distilled from CaH_2) (2.8 mL, 18 mmol) in dry THF (30 mL) held between −70 °C and −60 °C, whereupon a white precipitate formed. The suspension was warmed to −20 °C and then cooled back to −70 °C. A solution of 1,5,5-trimethylpyrrolidin-2-one (fractionally distilled from BaO) (2.3 mL, 17 mmol) in dry THF (25 mL) was added dropwise. The reaction mixture was warmed to 0 °C for 30 min, and then transferred dropwise via a cannula into a solution of hexachloroethane (4.17 g, 17.6 mmol) in dry THF (40 mL) held between −78 °C and −70 °C. After 1 h, the solution was warmed to rt and stirred for another 1 h. The solvent was removed and the residue taken up in CH_2Cl_2 (200 mL), and then filtered through diatomaceous earth several times until the solution was no longer cloudy. The solvent was removed and the residual yellow oil shaken with water (100 mL), causing separation of a white oil. The aqueous layer was decanted from this oil, filtered through diatomaceous earth, and extracted with $CHCl_3$ (100 mL × 2). The extracts were washed with brine (100 mL × 2) and dried to give a white waxy solid that was contaminated with 3-bromo-1,5,5-trimethylpyrrolidin-2-one (~13%). This byproduct could not be removed either by recrystallization (hexanes) or by sublimation (65 °C at 0.2 mmHg). Therefore, the solid was taken up in DMF (2 mL) and stirred with LiCl (510 mg, 12 mmol) for several hours. The mixture was diluted with water (10 mL), extracted into $CHCl_3$ (10 mL × 2), washed with brine (10 mL × 2), and dried to give white crystals which were triturated with cold hexanes to give **31** (1.12 g, 41%). mp 74–75 °C. HRMS-ESI (*m*/*z*): $[M+H]^+$ calcd for $C_7H_{13}ClNO$, 162.0686; found, 162.0691. ^{1}H NMR ($CDCl_3$): δ 4.45 (ddd, J = 8.4, 5.6, 0.4 Hz, 1H), 2.81 (s, 3H), 2.48 (dd, J = 14.0, 8.4 Hz, 1H), 2.17 (dd, J = 14.0, 5.6 Hz, 1H), 1.37 (s, 3H), 1.24 (s, 3H). ^{13}C NMR ($CDCl_3$): δ 169.2, 58.8, 53.9, 44.3, 26.5, 26.3, 24.9.

4.2.20. 3-Chloro-1-isopropylpyrrolidin-2-one (**32**)

This compound was synthesized in the same manner as **31** using 1-isopropylpyrrolidin-2-one (9.3 g, 73 mmol). The workup was modified slightly in that the reaction mixture was quenched with satd. $NaHCO_3$ (100 mL) and filtered through diatomaceous earth. The organic layer was separated off, and the aqueous layer

extracted with $CHCl_3$ (100 mL × 3). The combined extracts were washed with brine (300 mL × 2) and dried. The residual oil was worked up as for **31**. No brominated byproduct was present so the product was fractionally distilled (bp 68–70 °C at 0.9 mmHg) to give **32** as a colorless oil (8.2 g, 70%). HRMS-ESI (*m*/*z*): $[M+H]^+$ calcd for $C_7H_{13}ClNO$, 162.0686; found, 162.0690. ^1H NMR ($CDCl_3$): δ 4.38 (dd, *J* = 7.6, 4.4 Hz, 1H), 4.36 (sept, *J* = 6.8 Hz, 1H), 3.48 (ddd, *J* = −13.6, 6.8, 6.4 Hz, 1H), 3.32 (ddd, *J* = −13.6, 7.6, 4.0 Hz, 1H), 2.53 (dddd, *J* = −14.0, 7.6, 7.6, 6.4 Hz, 1H), 2.23 (dddd, *J* = −14.0, 7.6, 4.0, 4.0 Hz, 1H), 1.18 (d, *J* = 6.8 Hz, 3H), 1.16 (d, *J* = 6.8 Hz, 3H). ^{13}C NMR ($CDCl_3$): δ 169.4, 55.7, 43.4, 39.4, 29.8, 19.8, 19.4.

4.2.21. 1,5,5-Trimethyl-3-[2-(pyridin-2-yl)quinolin-4-yloxy] pyrrolidin-2-one (*33*)

2-(Pyridin-2-yl)-quinolin-4(1*H*)-one (222 mg, 1.00 mmol), **31** (210 mg, 1.40 mmol), and K_2CO_3 (866 mg, 6.28 mmol) in dry MeCN (35 mL) were heated to 80 °C for 70 h. The mixture was cooled to rt, poured into water (300 mL) and kept at 4 °C overnight. The precipitate that formed was recrystallized (hexanes–Et_2O) to give **33** as large white prisms (201 mg, 58%). mp 131–133 °C. HRMS-ESI (*m*/*z*): $[M+H]^+$ calcd for $C_{21}H_{22}N_3O_2$, 348.1712; found, 348.1712. ^1H NMR ($CDCl_3$): δ 8.72 (ddd, *J* = 4.8, 1,6, 0.8 Hz, 1H), 8.66 (d, *J* = 8.0 Hz, 1H), 8.26 (dd, *J* = 8.4, 0.8 Hz, 1H), 8.12 (s, 1H), 8.12 (d, *J* = 8.4 Hz, 1H), 7.90 (dt, *J* = 8.0, 2.0 Hz, 1H), 7.71 (ddd, *J* = 8.4, 6.8, 1.6 Hz, 1H), 7.50 (ddd, *J* = 8.4, 6.8, 1.2 Hz, 1H), 7.36 (ddd, *J* = 7.6, 4.8, 1.2 Hz, 1H), 5.40 (dd, *J* = 7.6, 5.6 Hz, 1H), 2.90 (s, 3H), 2.67 (dd, *J* = 13.6, 8.0 Hz, 1H), 2.19 (dd, *J* = 13.6, 8.0 Hz, 1H), 1.40 (s, 3H), 1.37 (s, 3H). ^{13}C NMR ($CDCl_3$): δ 169.3, 161.1, 157.2, 156.3, 149.1, 149.0, 136.9, 130.0, 129.2, 125.9, 124.1, 122.2, 121.9, 121.5, 99.5, 75.0, 58.3, 41.3, 27.3, 26.6, 24.6.

4.2..22. 1-Isopropyl-3-[2-(pyridin-2-yl)quinolin-4-yloxy] pyrrolidin-2-one (*34*)

2-(Pyridin-2-yl)-quinolin-4(1*H*)-one (222 mg, 1.00 mmol), **32** (160 μL, 1.12 mmol), and K_2CO_3 (834 mg, 6.03 mmol) in dry MeCN (35 mL) were heated to 80 °C for 7 d. The red mixture was cooled to rt, filtered through diatomaceous earth, taken up into CH_2Cl_2 (100 mL), washed with water (50 mL), and brine (50 mL × 2), and then dried. The product was isolated with HPLC [PFP column; MeOH–$NH_4CH_3CO_2$ buffer (25 mM, pH 7); 75:25] followed by trituration with aq MeOH (50% v/v) to give **34** as a white solid (167 mg, 48%). mp 108–110 °C. HRMS-ESI (*m*/*z*): $[M+H]^+$ calcd for $C_{21}H_{22}N_3O_2$, 348.1712; found, 348.1712. ^1H NMR ($CDCl_3$): δ 8.70 (ddd, *J* = 4.8, 1,6, 0.8 Hz, 1H), 8.66 (ddd, *J* = 8.0, 1.2, 1.2 Hz, 1H), 8.28 (dd, *J* = 8.4, 1.2 Hz, 1H), 8.14 (s, 1H), 8.10 (d, *J* = 8.4 Hz, 1H), 7.86 (dt, *J* = 8.0, 2.0 Hz, 1H), 7.71 (ddd, *J* = 8.4, 6.8, 1.2 Hz, 1H), 7.50 (ddd, *J* = 8.0, 6.8, 0.8 Hz, 1H), 7.34 (ddd, *J* = 7.2, 4.8, 1.2 Hz, 1H), 5.38 (dd, *J* = 7.6, 7.2 Hz, 1H), 4.50 (sept, *J* = 6.8 Hz, 1H), 3.48 (ddd, *J* = −13.2, 10.0, 3.6 Hz, 1H), 3.42 (ddd, *J* = −13.6, 7.2, 2.4 Hz, 1H), 2.83 (dddd, *J* = −13.6, 10.0, 7.6, 3.6 Hz, 1H), 2.26 (dddd, *J* = −13.6, 8.8, 7.2, 1.6 Hz, 1H), 1.26 (d, *J* = 6.8 Hz, 3H), 1.22 (d, *J* = 6.8 Hz, 3H). ^{13}C NMR ($CDCl_3$): δ 169.1, 161.2, 157.3, 156.3, 149.2, 148.9, 136.9, 130.0, 129.2, 125.9, 124.1, 122.3, 121.8, 121.5, 99.5, 75.9, 43.2, 38.5, 26.2, 19.8, 19.5.

4.2.23. 2-Nitro-N-(pyridin-2-ylmethyl)aniline (*35*)

2-(Aminomethyl)pyridine (4.9 mL, 48 mmol), 1-fluoro-2-nitrobenzene (5.5 mL, 52 mmol), and K_2CO_3 (13 g, 95 mmol) in DMF (35 mL) were heated for 19 h (90 °C, bath temp.). The blood red mixture was then allowed to cool, poured into citrate buffer (pH 7; 450 mL), and extracted with CH_2Cl_2 (250 mL × 2). The organic layer was then washed with water (350 mL × 5), followed by brine (350 mL), and then dried. The residue was sonicated in Et_2O (100 mL × 2), filtered through diatomaceous earth, and taken up into rapidly stirring hydrochloric acid (0.1 M; 500 mL). The biphasic mixture was filtered through diatomaceous earth, and the aqueous layer was separated off, washed with Et_2O (200 mL × 2), and neutralized with NH_4OH. The resultant precipitate was recrystallized twice (aq EtOH) to yield **35** as tiny golden needles (862 mg, 8%). mp 92–93 °C. HRMS-ESI (*m*/*z*): $[M+H]^+$ calcd for $C_{12}H_{12}N_3O_2$, 230.0930; found, 230.0937. ^1H NMR ($CDCl_3$): δ 8.87 (s, 1H), 8.64 (ddd, *J* = 4.8, 1.6, 0.8 Hz, 1H), 8.21 (dd, *J* = 8.4, 1.6 Hz, 1H), 7.68 (ddd, *J* = 7.6, 7.6, 1.6 Hz, 1H), 7.40 (ddd, *J* = 8.4, 6.8 Hz, 1H), 7.32 (d, *J* = 8.0 Hz, 1H), 7.23 (ddd, *J* = 7.6, 4.8, 0.8 Hz, 1H), 6.83 (dd, *J* = 8.4, 0.8 Hz, 1H), 6.68 (ddd, *J* = 8.4, 6.8, 1.2 Hz, 1H), 4.68 (d, *J* = 5.2 Hz, 1H). ^{13}C NMR ($CDCl_3$): δ 156.6, 149.6, 145.0, 136.9, 136.2, 132.4, 126.9, 122.6, 121.2, 115.8, 114.3, 48.4.

4.2.24. N-Isopropyl-N-methyl-2-(2-(pyridin-2-yl)-1H-benzo[d] imidazol-1-yloxy)propanamide (*36*)

NaH (480 mg, 2.00 mmol) in mineral oil (60% w/v) was added to a solution of **35** (229 mg, 1.00 mmol) in DMF (20 mL) at rt, which turned from bright yellow to deep red-brown. The solution was heated to 55 °C for 1 h. A solution of **16** (315 μL, 2.00 mmol) in DMF (5 mL) was then added and heating continued for another 1 h. The solution was then cooled and the solvent removed under reduced pressure. The residue was taken up into water (100 mL) and extracted with $CHCl_3$ (50 mL × 3). The combined extracts were then washed with water (50 mL) followed by brine (50 mL × 2), and then dried. The product was isolated with HPLC [PFP column; MeOH–NH_4HCO_2 buffer (25 mM, pH 7); 70:30] to give **36** as an orange syrup (240 mg, 71%). HRMS-ESI (*m*/*z*): $[M+H]^+$ calcd for $C_{19}H_{23}N_4O_2$, 339.1821; found, 339.1825. ^1H NMR ($CDCl_3$, *cis*–*trans*; 1.3:1.0): δ 8.76–8.73 (m, 2H, *cis* + *trans*), 8.32 (s, 1H, *cis*), 8.30 (s, 1H, *trans*), 7.90–7.85 (m, 2H, *cis* + *trans*), 7.76–7.72 (m, 3H, 2 *cis* + *trans*), 7.68 (m, 1H, *trans*) 7.41 (ddd, *J* = 7.6, 4.0, 1.2 Hz, 1H, *trans*), 7.40 (ddd, *J* = 7.6, 4.0, 1.2 Hz, 1H, *cis*), 7.35–7.28 (4H, 2 *cis* + 2 *trans*), 6.06 (q, *J* = 6.4 Hz, 1H, *trans*), 5.99 (q, *J* = 6.4 Hz, 1H, *cis*), 4.83 (sept, *J* = 6.8 Hz, 1H, *cis*), 4.13 (sept, *J* = 6.8 Hz, 1H, *trans*), 2.74 (s, 3H, *trans*), 2.60 (s, 3H, *cis*), 1.63 (d, *J* = 6.0 Hz, 3H, *cis*), 1.62 (d, *J* = 6.0 Hz, 3H, *trans*), 1.10 (d, *J* = 6.4 Hz, 3H, *trans*), 1.04 (d, *J* = 6.8 Hz, 3H, *cis*), 0.78 (d, *J* = 6.8 Hz, 3H, *cis*), 0.63 (d, *J* = 6.4 Hz, 3H, *trans*). ^{13}C NMR ($CDCl_3$): δ 169.5 (*cis*), 169.4 (*trans*), 149.2 (*cis*), 148.7 (*trans*), 147.3 (*trans*), 147.2 (*cis*), 137.8 (*cis* + *trans*), 136.9 (*cis* + *trans*), 133.7 (*trans*), 133.5 (*cis*), 124.7 (*trans*), 124.6 (*cis*), 124.3 (*cis* + *trans*), 123.3 (*cis* + *trans*), 120.2 (*trans*), 120.1 (*cis*), 111.1 (*cis*), 111.0 (*trans*), 80.8 (*cis*), 80.1 (*trans*), 47.7 (*trans*), 44.5 (*cis*), 27.8 (*cis*), 26.6 (*trans*), 20.8 (*trans*), 19.9 (*trans*), 19.3 (*cis*), 18.7 (*cis*), 16.8 (*trans*), 16.6 (*cis*).

4.3.. Radiochemistry

4.3.1. [^{11}C]Methyl triflate

[^{11}C]Methyl triflate was prepared from cyclotron-produced [^{11}C] carbon dioxide, via conversion into [^{11}C]methane by reduction with hydrogen over palladium, direct iodination of [^{11}C]methane, and passage of the generated [^{11}C]methyl iodide over heated silver triflate [46].

4.3.2. [^{11}C]**11**

Compound **19** (0.55 mg, 1.5 μmol) was treated with [^{11}C]methyl triflate in the presence of aq NaOH (0.5 M, 1 eq.) in dry MeCN (300 μL) at rt for 5 min. The radioligand was isolated with HPLC [XBridge column; MeCN–NH_4OH buffer (1 mM, pH 7.7); 65:35] at 6 mL/min (t_R = 11 min). The isolated product was taken up in ethanol–saline (10:90, v/v) containing polysorbate 80 (12 mg) and sterile filtered (Millex-MP 0.22 μm, 25 mm). The radiochemical purity of [^{11}C]**11** was >99% as established by HPLC [XBridge column; MeCN–NH_4HCO_2 buffer (0.1 M, pH 6.3); 50:50] at 2 mL/min (t_R = 9.2 min). Product identity was also confirmed by LC-MS of associated carrier. The average decay-corrected radiochemical yield of [^{11}C]**11** was 17% from cyclotron-produced [^{11}C]carbon dioxide and the average specific activity was 244 GBq/μmol at the end of

synthesis ($n = 7$), corresponding to about 40 min from the end of radionuclide production.

4.3.3. [^{11}C]**20**

Compound **18** (0.80 mg, 2.2 μmol) was treated with [^{11}C]MeOTf in the presence of excess NaH in dry MeCN (300 μL) at rt for 5 min The radioligand was isolated by HPLC [Luna column; MeCN–NH_4HCO_2 (0.1 mM); 45:55] at 6 mL/min ($t_R = 12$ min). The isolated product was formulated as for [^{11}C]**11**. HPLC analysis of [^{11}C]**20**, as for [^{11}C]**11**, showed > 99% radiochemical purity ($t_R = 6.1$ min). LC-MS of associated carrier confirmed product identity. The average decay-corrected radiochemical yield of [^{11}C]**20** was 21% from cyclotron-produced [^{11}C]carbon dioxide and the average specific activity was 126 GBq/μmol at the end of radiosynthesis ($n = 4$).

4.4. LogD determinations

These were performed on [^{11}C]**11** and [^{11}C]**20** of high radiochemical purity (>99.4%) by distribution between *n*-octanol and sodium phosphate buffer (pH 7.4, 0.15 M) at rt with the methodology that we have described previously [14]. Chemical stabilities of these radioligands in buffer were verified with HPLC. Neither radioligand was lost to adsorption during measurements.

4.5. Determination of ligand binding affinities for rat brain TSPO

All animal experiments were performed in accordance with the *Guide for the Care and Use of Laboratory Animals* and were approved by the NIMH Animal Care and Use Committee.

Binding assays were performed as previously described [27], except that crude rat brain homogenates were used instead of mitochondrial fractions. Binding data were analyzed with Prism 5 nonlinear regression curve-fitting software (GraphPad Prism; San Diego, CA). Briefly, whole rat brains from Sprague-Dawley rats were homogenized in cold HEPES buffer (50 mM; pH 7.4) with a Teflon pestle and Glas-Col Homogenizing System. The homogenates were centrifuged at 20,000*g* for 15 min at 4 °C. The pellets were then resuspended, aliquotted into various vials, and stored at −80 °C. A self-displacement assay on **1** was used as a control along with each assay of test ligand with [^{3}H]**1** as reference radioligand. The individually calculated control K_D values for **1** were compared to the reported value of 0.707 nM [27] as an assurance of the correctness of results obtained on test ligands. The K_D value of 0.707 nM for **1** was used as the dissociation constant to calculate K_i values for test ligands.

4.6. Pharmacological screening

Compound **11** was screened at the Psychoactive Drug Screening Program [51] for inhibition of binding at 10 μM concentration ($n = 4$) to a wide range of human receptors: α 1A, 1B, 1D, 2A, 2B and 2C; benzodiazepine; β_2; serotonin 1A, 1B, 1D, 1E, 2A, 2B, 2C, 3, 5A, 6, and 7; dopamine 2–5; opiate δ, κ, and μ; muscarinic 1–5; σ_1R and σ_2R; $GABA_A$; histamine 1 and 4; and human transporters (DAT, NET, SERT).

Conflict of interest

Each author declares there were not any actual or potential conflicts of interest that could have influenced this study.

Author contributions

This paper was composed with contributions from all authors. All authors approved the final version of the manuscript. CB synthesized and characterized the compounds; KJJ tested the ligands in vitro; SSZ measured the lipophilicities; CLM prepared the radioligands; RBI supervised in vitro tests; VWP initiated and supervised the project.

Acknowledgments

This study was supported by the Intramural Research Program of the National Institutes of Health (NIH), specifically the NIMH (projects ZIA MH0023793 and ZIAMH002852). We thank the NIH Clinical Center PET Department (Chief: Dr. Peter Herscovitch) for radioisotope production.

Appendix A. Supplementary data

Supplementary data related to this article can be found at http://dx.doi.org/10.1016/j.ejmech.2016.08.046.

References

[1] V. Papadopoulos, M. Baraldi, T.R. Guilarte, T.B. Knudsen, J.J. Lacapère, P. Lindemann, M.D. Norenberg, D. Nutt, A. Weizman, M.-R. Zhang, M. Gavish, Translocator protein (18kDa): new nomenclature for the peripheral-type benzodiazepine receptor based on its structure and molecular function, Trends Pharmacol. Sci. 27 (2006) 402–409.
[2] M.W. McEnery, A.M. Snowman, R.R. Trifiletti, S.H. Snyder, Isolation of the mitochondrial benzodiazepine receptor: association with the voltage-dependent anion channel and the adenine nucleotide carrier, Proc. Natl. Acad. Sci. U.S.A. 89 (1992) 3170–3174.
[3] A. Doble, C. Malgouris, M. Daniel, N. Daniel, F. Imbault, A. Basbaum, A. Uzan, C. Guérémy, G. Le Fur, Labelling of peripheral-type benzodiazepine binding sites in human brain with [^{3}H]PK 11195: anatomical and subcellular distribution, Brain Res. Bull. 18 (1987) 49–61.
[4] J. Benavides, D. Fage, C. Carter, B. Scatton, Peripheral type benzodiazepine binding sites are a sensitive indirect index of neuronal damage, Brain Res. 421 (1987) 167–172.
[5] D.R.J. Owen, P.M. Matthews, Imaging brain microglial activation using positron emission tomography and translocator protein-specific radioligands, in: P.C. Guest, S. Bahn (Eds.), Biomarkers of Neurological and Psychiatric Disease, vol. 101, Academic Press, Waltham, MA, 2011, pp. 19–39.
[6] J. Stefaniak, J. O'Brien, Imaging of neuroinflammation in dementia: a review, J. Neurol. Neurosurg. Psychiatry 87 (2016) 21–28.
[7] L. Vivash, T.J. O'Brien, Imaging microglial activation with TSPO PET: lighting up neurologic diseases? J. Nucl. Med. 57 (2016) 165–168.
[8] E. Setiawan, A.A. Wilson, R. Mizrahi, P.M. Rusjan, L. Miler, G. Rajkowska, I. Suridjan, J.L. Kennedy, P.V. Rekkas, S. Houle, J.H. Meyer, Role of translocator protein density, a marker of neuroinflammation, in the brain during major depressive episodes, JAMA Psychiatry 72 (2015) 268–275.
[9] B. Costa, E. Da Pozzo, C. Martini, Translocator protein as a promising target for novel anxiolytics, Curr. Top. Med. Chem. 12 (2012) 270–285.
[10] R. Camsonne, M.A. Moulin, C. Crouzel, A. Syrota, M. Mazière, D. Comar, Marquage au carbone 11 du PK11195 & visualisation des récepteurs périphériques des benzodiazepines par tomographie à émission positrons, J. Pharmacol. 17 (1986), 383–383.
[11] F. Shah, S.P. Hume, V.W. Pike, S. Ashworth, J. McDermott, Synthesis of the enantiomers of [*N*-methyl-^{11}C]PK 11195 and comparison of their behaviors as radioligands for PK binding sites in rats, Nucl. Med. Biol. 21 (1994) 573–581.
[12] J.C. Debruyne, K.J. Van Laere, J. Versijpt, F. De Vos, J.K. Eng, K. Strijckmans, P. Santens, E. Achten, G. Slegers, J. Korf, R.A. Dierckx, J.L. De Reuck, Semi-quantification of the peripheral-type benzodiazepine ligand [^{11}C]PK11195 in normal human brain and application in multiple sclerosis patients, Acta Neurol. Belg. 102 (2002) 127–135.
[13] A. Roivainen, K. Någren, J. Hirvonen, V. Oikonen, P. Virsu, T. Tolvanen, J.O. Rinne, Whole-body distribution and metabolism of [*N*-methyl-^{11}C](*R*)-1-(2-chlorophenyl)-*N*-(1-methylpropyl)-3-isoquinolinecarboxamide in humans; an imaging agent for in vivo assessment of peripheral benzodiazepine receptor activity with positron emission tomography, Eur. J. Nucl. Med. Mol. Imaging 36 (2009) 671–682.
[14] E. Briard, S.S. Zoghbi, M. Imaizumi, J.P. Gourley, H.U. Shetty, J. Hong, V. Cropley, M. Fujita, R.B. Innis, V.W. Pike, Synthesis and evaluation in monkey of two sensitive ^{11}C-labeled aryloxyanilide ligands for imaging brain peripheral benzodiazepine receptors in vivo, J. Med. Chem. 51 (2008) 17–30.
[15] M. Fujita, M. Imaizumi, S.S. Zoghbi, Y. Fujimura, A.G. Farris, T. Suhara, J. Hong, V.W. Pike, R.B. Innis, Kinetic analysis in healthy humans of a novel positron emission tomography radioligand to image the peripheral benzodiazepine receptor, a potential biomarker for inflammation, Neuroimage 40 (2008) 43–52.

[16] F. Yasuno, M. Ota, J. Kosaka, H. Ito, M. Higuchi, T.K. Doronbekov, S. Nozaki, Y. Fujimura, M. Koeda, T. Asada, T. Suhara, Increased binding of peripheral benzodiazepine receptor in Alzheimer's disease measured by positron emission tomography with [^{11}C]DAA1106, Biol. Psychiatry 64 (2008) 835–841.
[17] C.J. Endres, M.G. Pomper, M. James, O. Uzuner, D.A. Hammoud, C.C. Watkins, A. Reynolds, J. Hilton, R.F. Dannals, M. Kassiou, Initial evaluation of ^{11}C-DPA-713, a novel TSPO PET ligand, in humans, J. Nucl. Med. 50 (2009) 1276–1282.
[18] S.S.V. Golla, R. Boellaard, V. Oikonen, A. Hoffmann, B.N.M. van Berckel, A.D. Windhorst, J. Virta, M. Haaparanta-Solin, P. Luoto, N. Savisto, O. Solin, R. Valencia, A. Thiele, J. Eriksson, R.C. Schuit, A.A. Lammertsma, J.O. Rinne, Quantification of [^{18}F]DPA-714 binding in the human brain: initial studies in healthy controls and Alzheimer's disease patients, J. Cereb. Blood Flow Metab. 35 (2015) 766–772.
[19] L.P. Dickstein, S.S. Zoghbi, Y. Fujimura, M. Imaizumi, Y. Zhang, V.W. Pike, R.B. Innis, M. Fujita, Comparison of ^{18}F- and ^{11}C-labeled aryloxyanilide analogs to measure translocator protein in human brain using positron emission tomography, Eur. J. Nucl. Med. Mol. Imaging 38 (2011) 352–357.
[20] Q. Guo, A. Colasanti, D.R. Owen, M. Onega, A. Kamalakaran, I. Bennacef, P.M. Matthews, E.A. Rabiner, F.E. Turkheimer, R.N. Gunn, Quantification of the specific translocator protein signal of ^{18}F-PBR111 in healthy humans: a genetic polymorphism effect on in vivo binding, J. Nucl. Med. 54 (2013) 1915–1923.
[21] R. Mizrahi, P.M. Rusjan, J. Kennedy, B. Pollock, B. Mulsant, I. Suridjan, V. De Luca, A.A. Wilson, S. Houle, Translocator protein (18 kDa) polymorphism (rs6971) explains in-vivo brain binding affinity of the PET radioligand [^{18}F]-FEPPA, J. Cereb. Blood Flow Metab. 32 (2012) 968–972.
[22] A. Varrone, V. Oikonen, A. Forsberg, J. Joutsa, A. Takano, O. Solin, M. Haaparanta-Solin, S. Nag, R. Nakao, N. Al-Tawil, L.A. Wells, E.A. Rabiner, R. Valencia, M. Schultze-Mosgau, A. Thiele, S. Vollmer, T. Dyrks, L. Lehmann, T. Heinrich, A. Hoffmann, A. Nordberg, C. Halldin, J.O. Rinne, Positron emission tomography imaging of the 18-kDa translocator protein (TSPO) with [^{18}F] FEMPA in Alzheimer's disease patients and control subjects, Eur. J. Nucl. Med. Mol. Imaging 42 (2015) 438–446.
[23] P. Zanotti-Fregonara, Y. Zhang, K.J. Jenko, R.L. Gladding, S.S. Zoghbi, M. Fujita, G. Sbardella, S. Castellano, S. Taliani, C. Martini, R.B. Innis, F. Da Settimo, V.W. Pike, Synthesis and evaluation of translocator 18 kDa protein (TSPO) positron emission tomography (PET) radioligands with low binding sensitivity to human single nucleotide polymorphism rs6971, ACS Chem. Neurosci. 5 (2014) 963–971.
[24] W.C. Kreisl, K.J. Jenko, C.S. Hines, C.H. Lyoo, W. Corona, C.L. Morse, S.S. Zoghbi, T. Hyde, J.E. Kleinman, V.W. Pike, F.J. McMahon, R.B. Innis, Biomarkers Consortium PET Radioligand Project Team, A genetic polymorphism for translocator protein 18 kDa affects both in vitro and in vivo radioligand binding in human brain to this putative biomarker of neuroinflammation, J. Cereb. Blood Flow Metab. 33 (2013) 53–58.
[25] D.R.J. Owen, R.N. Gunn, E.A. Rabiner, I. Bennacef, M. Fujita, W.C. Kreisl, R.B. Innis, V.W. Pike, R. Reynolds, P.M. Matthews, C.A. Parker, Mixed-affinity binding in humans with 18-kDa translocator protein ligands, J. Nucl. Med. 52 (2011) 24–32.
[26] V.W. Pike, Considerations in the development of reversibly binding PET radioligands for brain imaging, Curr. Med. Chem. 23 (2016) 1818–1869.
[27] C. Brouwer, K. Jenko, S.S. Zoghbi, R.B. Innis, V.W. Pike, Development of *N*-methyl-(2-arylquinolin-4-yl)oxypropanamides as leads to PET radioligands for translocator protein (18 kDa), J. Med. Chem. 57 (2014) 6240–6251.
[28] M.D. Shultz, Setting expectations in molecular optimizations: strengths and limitations of commonly used composite parameters, Bioorg. Med. Chem. Lett. 23 (2013) 5980–5991.
[29] E. Frérot, J. Coste, A. Pantaloni, M.-N. Dufour, P. Jouin, PyBOP and PyBroP: two reagents for the difficult coupling of the α,α-dialkyl amino acid, Aib, Tetrahedron 47 (1991) 259–270.
[30] C.P. Jones, K.W. Anderson, S.L. Buchwald, Sequential Cu-catalyzed amidation-base-mediated Camps cyclization: a two-step synthesis of 2-aryl-4-quinolones from *o*-halophenones, J. Org. Chem. 72 (2007) 7968–7973.
[31] A.G. Osborne, L.A.D. Miller, Regioselective alkoxydehalogenation of 2,4-dihalogenoquinolines and a reinvestigation of the bromination of 2-methoxyquinoline, J. Chem. Soc. Perkin Trans. 1 (1993) 181–184.
[32] W. Czuba, M. Woźniak, Różnice w zdolności do wymiany nukleofilowej chlorowców podstawionych w położeniu 2 i 4 1,8-naftyrydyny, Zesz. Nauk. Uniw. Jagielloń. Pr. Chem. 20 (1975) 61–70.
[33] H. M'rabet, S. M'hirsi, H. Zantour, B. Baccar, Action de quelques réactifs électrophiles sur les *N*-aryl acétimidates, J. Soc. Chim. Tunis. 3 (1994) 513–521.
[34] P. Actor, C.E. Berkoff, P.N. Craig, M. Julius, G. Redl, R.J. Grout, B.M. Hynam, M.W. Partridge, Antimicrobial 2-amino-4-alkoxyquinolines: synthesis and analysis of structure-activity correlations, Arzneim. Forsch. 24 (1974) 8–11.
[35] N. Clauson-Kaas, Z. Tyle, Preparation of *cis* and *trans* 2,5-dimethoxy-2-(acetamidomethyl)-2,5-dihydrofuran, of *cis* and *trans* 2,5-dimethoxy-2-(acetamidomethyl)-tetrahydrofuran and of 1-phenyl-2-(acetamidomethyl)-pyrrole, Acta Chem. Scand. 6 (1952) 667–670.
[36] A.K. Beck, M.S. Hoekstra, D. Seebach, 1,3-Diketones by 1:1-reactions of Li-enolates with acid chlorides generation of kinetic enolates with mesityl lithium, Tetrahedron Lett. 18 (1977) 1187–1190.
[37] E. Vedejs, R.J. Galante, P.G. Goekjian, A thio-Diels–Alder route to the azocine ring system. Total synthesis of (±)-otonecine, J. Am. Chem. Soc. 120 (1998) 3613–3622.
[38] G.W. Stacy, B.V. Ettling, A.J. Papa, Reactions of benzaldehyde with *o*-nitroaniline, J. Org. Chem. 29 (1964) 1537–1540.
[39] S. Takahashi, H. Kanō, Benzimidazole *N*-oxides. I. The structure of benzimidazole *N*-oxide and synthesis of its derivatives, Chem. Pharm. Bull. 11 (1963) 1375–1381.
[40] L. Cai, S. Lu, V.W. Pike, Chemistry with [^{18}F]fluoride ion, Eur. J. Org. Chem. (2008) 2853–2873.
[41] S. Preshlock, M. Tredwell, V. Gouverneur, ^{18}F-Labeling of arenes and heteroarenes for applications in positron emission tomography, Chem. Rev. 116 (2016) 719–766.
[42] A. Cappelli, M. Anzini, S. Vomero, P.G. De Benedetti, M.C. Menziani, G. Giorgi, C. Manzoni, Mapping the peripheral benzodiazepine receptor binding site by conformationally restrained derivatives of 1-(2-chlorophenyl)-*N*-methyl-*N*-(1-methylpropyl)-3-isoquinolinecarboxamide (PK11195), J. Med. Chem. 40 (1997) 2910–2921.
[43] Y.-S. Lee, F.G. Siméon, E. Briard, V.W. Pike, Solution structures of the prototypical 18 kDa translocator protein ligand, PK 11195, elucidated with ^{1}H/^{13}C NMR spectroscopy and quantum chemistry, ACS Chem. Neurosci. 3 (2012) 325–335.
[44] Ł. Jaremko, M. Jaremko, K. Giller, S. Becker, M. Zweckstetter, Structure of the mitochondrial translocator protein in complex with a diagnostic ligand, Science 343 (2014) 1363–1366.
[45] G. Primofiore, F. Da Settimo, S. Taliani, F. Simorini, M.P. Patrizi, E. Novellino, G. Greco, E. Abignente, B. Costa, B. Chelli, C. Martini, *N,N*-Dialkyl-2-phenylindol-3-ylglyoxylamides. A new class of potent and selective ligands at the peripheral benzodiazepine receptor, J. Med. Chem. 47 (2004) 1852–1855.
[46] D.M. Jewett, A simple synthesis of [^{11}C]methyl triflate, Appl. Radiat. Isot. 43 (1992) 1383–1385.
[47] C.A. Bischoff, Studien über Verkettungen. XXVI. Das Aethylanilin, Ber. Dtcsh. Chem. Ges. 30 (1897) 3178–3180.
[48] M. Pohmakotr, C. Winotai, α-Hydroxylation of carboxylic acids and amides using bis(trimethylsilyl)peroxide, Synth. Commun. 18 (1988) 2141–2146.
[49] P.D. Williams, D.S. Perlow, L.S. Payne, M.K. Holloway, P.K.S. Siegl, T.W. Schorn, R.J. Lynch, J.J. Doyle, J.F. Strouse, G.P. Vlasuk, K. Hoogsteen, J.P. Springer, B.L. Bush, T.A. Halgren, A.D. Richards, J. Kay, D.F. Veber, Renin inhibitors containing conformationally restricted P_1-P_1' dipeptide mimetics, J. Med. Chem. 34 (1991) 887–900.
[50] E.P. Kramarova, A.G. Shipov, N.A. Orlova, O.B. Artamkina, I.Y. Belavin, Y.I. Baukov, Simple method for the *N*-alkylation of lactams, J. Gen. Chem. USSR 58 (1988) 970–979.
[51] J. Besnard, G.F. Ruda, V. Setola, K. Abecassis, R.M. Rodriguiz, X.-P. Huang, S. Norval, M.F. Sassano, A.I. Shin, L.A. Webster, F.R.C. Simeons, L. Stojanovski, A. Prat, N.G. Seidah, D.B. Constam, G.R. Bickerton, K.D. Read, W.C. Wetsel, I.H. Gilbert, B.L. Roth, A.L. Hopkins, Automated design of ligands to polypharmacological profiles, Nature 492 (2012) 215–220.